

# Semiparametric Estimation of Target Location in Wireless Sensor Network

by

Nirupam Chakrabarty

A dissertation submitted in partial fulfillment  
of the requirements for the degree of  
Doctor of Philosophy  
(Statistics)  
in The University of Michigan  
2014

Doctoral Committee:

Professor Moulinath Banerjee, co-Chair  
Professor George Michailidis, co-Chair  
Professor Bin Nan  
Associate Professor Stilian Stoev



© Nirupam Chakrabarty 2014  
All Rights Reserved

## ACKNOWLEDGEMENTS

First and foremost, I would like to sincerely thank my advisors Prof. Moulinath Banerjee and Prof. George Michailidis for their continuous support and guidance throughout my PhD program. I am also grateful to my parents and my wife Adita for their support and encouragement. I am also thankful to Prof. Bin Nan and Prof. Guang Cheng for their valuable suggestions and guidance which helped me a lot. Finally, I take this opportunity to thank all the distinguished Professors and friends at University of Michigan whose valuable comments and suggestions helped me a lot not only in my thesis, but also understanding the current research work going on in different branches of statistics.

# TABLE OF CONTENTS

<b>ACKNOWLEDGEMENTS</b> . . . . .	ii
<b>LIST OF FIGURES</b> . . . . .	v
<b>LIST OF TABLES</b> . . . . .	vii
<b>LIST OF APPENDICES</b> . . . . .	viii
<b>ABSTRACT</b> . . . . .	ix
<b>CHAPTER</b>	
<b>I. Introduction</b> . . . . .	1
1.1 Related Work . . . . .	3
1.2 Outline of the Thesis . . . . .	6
<b>II. Semiparametric Target Estimation Based on Isotropic Signal</b>	9
2.1 Introduction . . . . .	9
2.1.1 Impact of Signal Misspecification: . . . . .	11
2.2 Problem Formulation and Estimation Methods . . . . .	14
2.2.1 One-stage Isotonic Regression . . . . .	14
2.2.2 Two-stage Estimation Method for Target Detection . . . . .	15
2.2.3 Ellipsoidal confidence region based on Bootstrap: . . . . .	19
2.3 Challenges with Boundary Points and a Modified Algorithm . . . . .	20
2.4 Performance Evaluation . . . . .	21
2.5 Applications - The ZebraNet Project . . . . .	23
2.5.1 Robustness to Model Misspecification . . . . .	27
2.6 Theoretical Issues . . . . .	28
<b>III. Target Estimation Based on Anisotropic Signal</b> . . . . .	31
3.1 Introduction . . . . .	31

3.2	Problem Formulation and Estimation Methods . . . . .	34
3.2.1	Ellipsoidal confidence region based on Subsampling:	39
3.3	Performance Evaluation . . . . .	40
3.3.1	Comparison with Isotonic Regression Method . . . . .	43
3.4	Applications - The ZebraNet Project . . . . .	48
3.5	Theoretical Issues . . . . .	52
<b>IV. Kernel-based Target Estimation for Isotropic Signal . . . . .</b>		<b>54</b>
4.1	Introduction . . . . .	54
4.2	Estimation Methods in One-dimension . . . . .	56
4.3	Performance Evaluation . . . . .	57
4.4	Theoretical Issues and Conclusion . . . . .	58
<b>APPENDICES . . . . .</b>		<b>60</b>
<b>BIBLIOGRAPHY . . . . .</b>		<b>66</b>

## LIST OF FIGURES

<u>Figure</u>		
2.1	Plot of 1-dimensional Signal Functions with target at 2.5 . . . . .	13
2.2	Plot of an exponential signal over unit square with target at (0.5, 0.5) and (0.9, 0.1) . . . . .	16
2.3	Finding high signal circular region in stage 1, using piecewise constant model . . . . .	18
2.4	Plot of exponential signal and exponential (spike) signal with target at (2.5, 2.5) . . . . .	23
2.5	Locations of the zebra in study period . . . . .	26
2.6	Two-Stage Confidence Region of zebra location at six time points based on Exponential Signal . . . . .	27
2.7	Two-Stage Confidence Region of zebra location at six time points, based on Anisotropic Signal . . . . .	29
3.1	Plot of Ellipsoidal Contours formed by Sensors for Polynomial Signal Model with $\rho = 0.5, 0.8$ . . . . .	33
3.2	Ellipsoidal Contours Formed by Sensors Receiving Similar Signals, obtained by Clustering, with Target at (2.5, 2.5) . . . . .	35
3.3	Plot of $B(k)/TSS$ over $k$ and the "elbow" point . . . . .	37
3.4	Finding No. of Informative Clusters with target at (2.5, 2.5) . . . . .	39
3.5	Plot of Exponential Signals with Different Noise Levels . . . . .	41

3.6	Plot of Exponential and Exponential(spike) signals for target at (2.5, 2.5) . . . . .	42
3.7	Plot of Exponential and Exponential(spike) signals for target at (1, 1)	42
3.8	Plot of informative clusters for Exponential Signal Model with $\rho = 0.5$	46
3.9	Plot of informative clusters for Exponential Signal Model with $\rho = 0.8$	46
3.10	Confidence Region of zebra location at six time points, based on Method 1 (Unweighted Mean) . . . . .	52
3.11	Confidence Region of zebra location at six time points, based on Method 2 (Weighted Mean) . . . . .	53
B.1	Histogram and QQplot of $\sqrt{n}(\hat{\theta} - \theta_0)$ for 1d Exponential Model, $n=2000$	62
B.2	Histogram and QQplot of $\sqrt{n}(\hat{\theta} - \theta_0)$ for 1d Polynomial Model, $n=2000$	63
C.1	Histogram and QQplot of $\sqrt{n}(\hat{\theta}_1 - \theta_{10})$ for 2d Exponential Model, $n=5000, \rho = 0.5$ . . . . .	64
C.2	Histogram and QQplot of $\sqrt{n}(\hat{\theta}_2 - \theta_{20})$ for 2d Exponential Model, $n=5000, \rho = 0.5$ . . . . .	65



## LIST OF TABLES

### Table

2.1	Comparison between misspecified parametric and semiparametric estimation . . . . .	13
2.2	2-dim Simulation Results with target at (2.5,2.5) . . . . .	24
2.3	2-dim Simulation Results with target at (1,1) . . . . .	25
2.4	Performance of One-stage and Two-stage methods at zebra tracking, based on Exponential Signal . . . . .	28
3.1	Simulation Results for Anisotropic Models with target at (2.5,2.5), Using Isotonic Estimation Method . . . . .	33
3.2	2-dim Simulation Results with target at (2.5,2.5) . . . . .	44
3.3	2-dim Simulation Results with target at (1,1) . . . . .	45
3.4	Comparison of Methods for Isotropic signal with target at (2.5,2.5) .	49
3.5	Comparison of Ellipse and Circle Fitting in Clustering based Method for Isotropic signal with target at (2.5,2.5) . . . . .	50
3.6	Performance of Clustering method at zebra tracking, based on Polynomial Signal . . . . .	52
4.1	1-dim Simulation Results with target at (2.5) . . . . .	58
4.2	1-dim Simulation Results with target at (1) . . . . .	59

## LIST OF APPENDICES

### Appendix

A.	Isotonic Regression . . . . .	61
B.	Plots for One-stage Isotonic Estimate . . . . .	62
C.	Plots for Clustering based Estimate for Exponential Model . . . . .	64

# ABSTRACT

Semiparametric Estimation of Target Location in Wireless Sensor Network

by

Nirupam Chakrabarty

Co-Chair: Moulinath Banerjee, George Michailidis

Wireless sensor networks are widely used for monitoring natural phenomena in space and over time, as well as for target detection and tracking. In a target detection setting, sensors acquire signals emitted from the target, corrupted by background noise, and decisions are made on the presence and exact location of the target. Often, the signal propagation model is unknown in practice, as it depends on the type of target present in the monitored region. There is a rich literature on detection/tracking frameworks based on parametric signal propagation models, which are not particularly robust to misspecification. In this thesis, we introduce a few semiparametric methods of estimating the target location which does not rely on the form of the signal propagation model, and hence overcomes such issues. Further, the proposed framework for isotropic signal models incorporates a two-stage signal acquisition design that enables the utilization of only a small number of available sensors, thus reducing energy and communications costs. Both simulation studies and data examples demonstrate the utility and robustness of the proposed methods for isotropic and anisotropic signal models.

# CHAPTER I

## Introduction

Detection, identification and tracking of spatial phenomena are important tasks in various environmental and infrastructure applications (Veeravalli and Varshney (2012)). In general, sensor networks are built from small, inexpensive devices that have short-range sensing capabilities and limited computational and communication capacity (Sohraby, et al. (2007)). These networks offer the capability of densely covering a large area, but at the same time are constrained by the limiting sensing, processing and power capabilities of the sensors. In target detection and tracking applications, sensors acquire signals emitted from the target that are corrupted by background noise, and initially make individual decisions about the presence/absence of the target. The signals are typically some energy readings from the environment, which could be temperature, acoustic signal, vibration, etc. The task of the network is to efficiently use the available data in order to estimate and track the object of interest. For example, in areas and facilities surveillance monitoring (Estrin (2006)), the task is to detect an intrusion and follow its path; in habitat monitoring (Mainwaring et al. (2002)), to identify and track herds; in environmental monitoring (Padhy et al. (2005)), to estimate soil moisture levels (Cardell-Oliver et al. (2005)), dispersion of pollutants (Kim et al. (2006)), etc. Other recent applications of wireless sensor networks include identification of chemical, biological, radiological, nuclear and

explosive phenomena, infrastructure monitoring (Xu et al. (2004)), active volcano monitoring (Werner-Allen et al. (2006)), cane-toad monitoring (Hu et al. (2009)), sensing in high alpine environments (Keller et al. (2009)), detection and localization of hidden radioactive sources (Wan et al. (2012)), forest fire detection (Bouabdellah et al. (2013)), and landslide detection (Ramesh et al. (2009)).

In order to carry out these tasks, the physical characteristics of the sensors and the constraints imposed by the technology must be taken into consideration. Typically, sensors are autonomously powered devices capable of collecting measurements of one or more types (e.g acoustic, infrared, etc.). The problem we address here is that of estimating a target's location based on signal strengths received by the sensors deployed in a wireless sensor network. In general, the problem is formulated as follows: consider  $N$  identical sensors deployed at locations  $x_i, i = 1, 2, \dots, N$  over a two-dimensional monitoring region  $R$ . A target at location  $\theta = (\theta_x, \theta_y) \in R$  emits a signal which is captured by the deployed sensors. Specifically, let  $Y_i = S_i + \epsilon_i, i = 1, 2, \dots, N$  denote the energy measured by the  $i$ -th sensor, where  $S_i \equiv S_i(\theta)$  is the signal of the target measured at location  $i$ , and  $Y_i$  is  $S_i$  contaminated by i.i.d random noise  $\epsilon_i$ . Given such measurements, typical tasks performed by the sensor network include detection of presence of a target, followed by identification of its location and finally tracking over time (Sohraby, et al. (2007)). Key constraints that sensor networks routinely face relate to limited energy availability, memory, computational speed and communications bandwidth. Hence, there is a rich signal processing literature addressing these issues (see Anastasi et al. (2009) and references therein).

The wireless sensor network accomplishes these objectives by collecting the available measurements from the sensors and processing them appropriately. The information fusion occurs at a central location, called the fusion center. The information trans-

mitted to the fusion center can be either the energy measurements  $E_i$  themselves or binary decisions  $Y_i = I(E_i \geq \tau_i)$  determined by a pre-specified threshold  $\tau_i$  related to the individual sensors false alarm probability, with  $I(\cdot)$  denoting the indicator function. The former approach is called value fusion, and the latter decision fusion (see Katenka et al. (2008)). In general, value fusion is more accurate in terms of detection probability and localization, but decision fusion is more economical due to lower communication cost of one-bit transmissions and proves more robust in noisy environments. Here we focus on a value fusion situation, where the energy measurements  $E_i$  themselves are transmitted to the fusion center so that there is no loss of data in the process. Here our goal is to efficiently estimate the location of the target based on the energy readings from the sensors deployed.

## 1.1 Related Work

The classical approach to the target detection problem is to assume a specific model for the signal and frame it as a hypothesis test where the null hypothesis:  $H_0$ : no target is present vs. the alternative  $H_1$ : there is a target in the field (see Viswanathan et al. (1997) for a comprehensive review). This approach was used by fusion algorithms developed in the 1980's with applications to surveillance systems (e.g. radars, see Abdel-Samad and Tewfik (1999)). Also optimal decision rules based on classical Bayesian decision theory have been worked out when both the signal and noise distributions are known, for independent and correlated decisions (Wang et al. (2006)). However in most practical situations, the assumption of a known signal model can be restrictive, since different types of targets can emit different types of signals.

The canonical signal processing problems of target detection, localization and tracking

over time have received an increasing degree of attention over the last few years. The literature on these problems goes back to radar systems (Abdel-Samad and Tewfik, 1999), where localization was mostly performed via beam-forming methods. Existing localization algorithms for wireless sensor networks can be broadly divided into two general classes: those based on actual energy readings  $E_i$  (Kaplan et al., 2001; Li et al., 2002; Sheng and Hu, 2003; Blatt and Hero, 2006) and those based on binary decisions  $Y_i$  (Niu and Varshney, 2004; Noel et al., 2006; Ermis and Saligrama, 2006). Li et al. (2002) used non-linear least squares to localize the target, assuming an isotropic exponentially decaying signal model. For acoustic energy measurements, a maximum likelihood (ML) estimation method based on the Expectation-Maximization (EM) algorithm and a projection solution for the problem of target localization was proposed by Sheng and Hu (2003). The EM algorithm was used to fit the mixture model for energies coming from multiple targets. These methods proved to be more accurate than nonlinear least square estimates, but computationally more demanding. Compared to techniques that depend on such physical variables as direction of arrival (DOA) and time delay of arrival (TDOA) (Kaplan et al., 2001; Chen et al., 2002; Meesookho and Narayanan, 2005), energy based methods do not require a very accurate synchronization among the sensors and provide accurate estimation of target locations. However, energy-based techniques require transmission of real value data from all the sensors, which may not be always feasible under communication constraints. Moreover, the methods of Sheng and Hu (2003) require transmission of the mean and variance of the background noise, which often are unknown and may have to be estimated together with the target location and signal amplitude. Options for reducing communications cost include implementation of an optimization-based localization algorithm in a distributed manner (Blatt and Hero, 2006), or obtaining energy information only from cluster heads rather than all sensors (Zou and Chakrabarty, 2003).

Binary decision transmission offers significant cost savings, since only positive one-bit detection notifications are sent to the fusion center. Niu and Varshney (2004) developed maximum likelihood target location estimation from binary and multi-bit discrete data, along with the corresponding Cramer-Rao bound. The MLE approach reduces the problem of localization to that of non-linear function optimization, which may suffer from existence of local maxima, slow convergence rate and high computational complexity. Noel et al. (2006) proposed an improved MLE approach using the same likelihood as Niu and Varshney (2004) maximized by particle swarm optimization techniques, which was shown to outperform deterministic quasi Newton-Raphson schemes. Another recent approach used distributed false discovery rate to select the most informative sensors to communicate with the fusion center, although it relies on multiple within network communications on each step of the localization (Ermis and Saligrama, 2006). Also recently, Katenka et al. (2008) proposed local vote decision fusion (LVDF) algorithm, in which each sensor adjusts its initial binary decision of presence of a target according to a majority vote by the other sensors in its neighborhood. The updated decisions are then communicated to the fusion center which makes the final decision. Detection procedures for LVDF were developed in Katenka et al. (2006), where it was shown that the de-noising effect of LVDF leads to a robust procedure for target detection, particularly in noisy environments with low signal-to-noise ratio. LVDF also reduces the overall communication costs since by canceling out false positives, it reduces the number of positive decisions which need to be communicated to the fusion center. Other related papers include target localization in relation to the coverage problem (Wang et al., 2005), and a Bayesian approach to target localization and sensor selection and placement (Wang et al., 2006).

So far, none of the above approaches has dealt with the problem of target detection in a non-parametric way. When detecting a target location based on the signals



received by sensors, most of the methods developed so far are based on a particular form of the signal generating model which might not be applicable to different types of signals emitted from different type of targets. In this thesis, we intend to analyze the problem of target detection from a non-parametric point of view, without assuming any particular form of the signal generating process.

## 1.2 Outline of the Thesis

In this thesis, we consider the problem of estimating the target location in a wireless sensor network from a semiparametric point of view. In many practical scenarios, the type of the target present would not be known in advance, so the assumption of a known signal model can be restrictive and quite ambitious. In fact, in Chapter II, we demonstrate the effect of parametric estimation based on a mis-specified parametric signal model. Throughout the course of this thesis, we develop algorithms which do not depend on a particular known parametric signal model and thus can be applied to a wide range of different signal models.

In Chapter II, we develop algorithms to effectively estimate the target location for isotropic signal models, where the signal decays uniformly in each direction from the target location. In this case, the signal received by a sensor would only be a function of the Euclidean distance between the sensor and the target present, as a result, the sensors capturing similar signal strengths would form circular contours with the center being the true target location. The signal received can then be modeled as:  $Y_i = g_0(\|x_i - \theta_0\|) + \epsilon_i, i = 1, 2, \dots, N$ , where  $x_i \in \mathbb{R}^2$  is the known location of  $i$ -th sensor,  $\theta_0$  is the unknown location of the target and  $g_0$  is an unknown monotone decreasing function. Also,  $\epsilon_i, i = 1, 2, \dots, N$  are the i.i.d random noises. Our primary goal is to estimate  $\theta_0$ , which will also necessitate some estimation of  $g_0$  in this case. Note that the above model is a special case of ‘*bundled* parameters’ problem – the

nuisance parameter  $g_0$  contains the parameter of interest  $\theta_0$  as part of its argument – which is well-known to be notoriously difficult, especially without using smoothing techniques for estimating  $g_0$ . We develop algorithms based on isotonic regression to effectively estimate the target location and construct relevant confidence region. We also develop a two-stage signal acquisition design that enables the utilization of only a small number of available sensors, thus reducing energy and communications costs. The performance of the proposed algorithms is demonstrated through simulation results and real data applications. A major methodological advantage of our approach is the use of isotonic regression which does not require a smoothing parameter, thereby simplifying the implementation of our procedure considerably. Kernel or spline based procedures, though theoretically more tractable, have to deal with a tuning parameter, practical choices for which can often be tricky (Heidenreich et al. (2013)).

However, in many practical cases, the signal propagation model may not be isotropic in nature. In these cases, the signal strength decays at different rate in different directions, making the target estimation more challenging. The algorithms developed for isotropic models in Chapter II may perform poorly for anisotropic signal models, as those methods depend heavily on the isotropic property of the signal propagation model. In Chapter III, we consider anisotropic signal models which form ellipsoidal contours for sensors capturing similar signal strengths. The signal received can then be modeled as:  $Y_i = g_0 \left( (x_i - \theta_0)^T \Sigma^{-1} (x_i - \theta_0) \right) + \epsilon_i, i = 1, 2, \dots, N$ , where  $x_i \in \mathbb{R}^2$  is the known location of  $i$ -th sensor,  $\theta_0$  is the unknown location of the target,  $\Sigma$  is an unknown symmetric matrix which controls the shape and alignment of the ellipsoidal contours and  $g_0$  is an unknown monotone decreasing function. As before, our primary goal is to estimate  $\theta_0$ , the true location of the target present. In Chapter III, we develop a clustering based algorithm to effectively estimate the location of the target

and produce relevant confidence region for anisotropic signal models, without directly estimating the signal generating function  $g_0$ . Again, the performance of the proposed algorithm is demonstrated through simulation results and real data applications. A major advantage of our method is that we do not need to directly estimate the signal function  $g_0$  in this case, which can be tricky specially for anisotropic signal models.

Recall that in Chapter II, we propose an isotonic regression based method for isotropic signal model where the parametric estimate of  $\theta_0$  is obtained based on a non-smooth isotonic estimate of the non-parametric function  $g_0$ . In recent years, there have been some significant developments in theoretical front for semiparametric *bundled* parameter problems, where the non-parametric function is estimated using a smooth function. For example, Ichimura and Lee (2010) have studied the asymptotic properties of semiparametric M-estimators and they have established that the asymptotic distribution of the parametric estimate is Gaussian under certain regularity conditions on the estimate of the non-parametric part. Also Ding and Nan (2012) have recently used a spline based approach for estimation in the semiparametric linear regression model with right censored data and have established an asymptotic normal distribution of the parametric component, under certain regularity conditions. Getting motivated by these recent developments, we revisit the problem of target estimation based on isotropic signal model in Chapter IV and propose a kernel-based method to produce a smooth estimate of the unknown signal function  $g_0$ , and subsequently estimate target location  $\theta_0$ . This method will be theoretically more tractable than the isotonic regression based method developed in Chapter II. However, the kernel-based method involves selecting a tuning parameter like the bandwidth of the kernel function, which can be tricky at times. Initial simulation results show satisfactory performance of the kernel based method, but theoretical properties of the estimate will be a topic of future research.

## CHAPTER II

# Semiparametric Target Estimation Based on Isotropic Signal

### 2.1 Introduction

As discussed in Chapter I, wireless sensor networks are used broadly for detection, identification and tracking of spatial phenomena in various environmental and infrastructure applications. In most cases, sensors acquire signals emitted from the target that are corrupted by noise and initially make individual decisions about the presence/absence of the target. The signals are typically some energy readings from the environment, like temperature readings, acoustic signals, vibration etc. The main objective of sensor network is to effectively use the available data to track and monitor the object of interest. Recent applications of wireless sensor networks include identification of chemical, biological, radiological, nuclear and explosive phenomena, infrastructure monitoring (Xu et al. (2004)), active volcano monitoring (Werner-Allen et al. (2006)), cane-toad monitoring (Hu et al. (2009)), sensing in high alpine environments (Keller et al. (2009)), detection and localization of hidden radioactive sources (Wan et al. (2012)), forest fire detection (Bouabdellah et al. (2013)), and landslide detection (Ramesh et al. (2009)).

As discussed before, the wireless sensor network accomplishes these objectives by collecting the available measurements from the sensors and processing them appropriately. The information fusion usually occurs at a central location (fusion center), although there is extensive work for distributed processing of the data (see Iyengar and Brooks (2012) and references therein). The information transmitted to the fusion center can be either the energy measurements  $Y_i$  themselves or in order to reduce communications overhead, binary decisions of the form  $Z_i = I(Y_i \geq \tau_i)$  determined by a pre-specified threshold  $\tau_i$  related to the individual sensors false alarm probability, with  $I(\cdot)$  denoting the indicator function (Katenka et al. (2008)). In general, transmitting energy measurements leads to more accurate target detection and localization. In this thesis, we focus on transmission of energy measurements  $Y_i$  without assuming a *known parametric* form for the signals emitted by the target. In addition, in order to restrict energy consumption, we adopt a two-stage data acquisition and processing strategy. Specifically, throughout the monitoring period only a small number of sensors is active; once a target has been detected and a rough estimate of its location provided, *additional* sensors in a small vicinity of the first-stage target estimate are activated and acquire additional energy measurements and thus a final target location is obtained. As numerical experiments in Section 2.5 suggest, the *effective* number of sensors used to track an animal target ranges between 35-50% of the total number of available sensors, depending on the location of the target in the monitored region. At the same time, the proposed two-stage estimation procedure achieves significant gains in statistical efficiency ranging from 15-45% in terms of target coverage probabilities.

In most of the literatures, the form of the signal generating model is assumed to be known (e.g exponential/polynomial etc) and the subsequent analysis is based on that assumption. But the assumption of a known signal model can be restrictive and quite

ambitious, since there may be different types of targets present, whose signals follow different models. In this chapter, we take a less restrictive (non-parametric) approach to tackle the problem of target estimation. We only assume that the signal strength received by the sensor is isotropic in nature and is a decreasing function of the distance between the target and the sensor, a practical assumption in almost all real life scenarios. The signal received can then be modeled as:  $Y_i = g_0(\|x_i - \theta_0\|) + \epsilon_i, i = 1, 2, \dots, N$ , where  $x_i$  is the known location of  $i$ -th sensor,  $\theta_0$  is the unknown location of the target,  $g_0$  is an unknown monotone decreasing function and  $\|\cdot\|$  is the  $L^2$  norm. As before,  $\epsilon_i, i = 1, 2, \dots, N$  are the i.i.d random noises. Our primary goal is to estimate  $\theta_0$ , which as will be seen shortly will also necessitate some estimation of  $g_0$ : indeed, a key idea in this chapter is to facilitate the estimation of  $\theta_0$  by exploiting the monotone decreasing property of  $g_0$  which enables the use of isotonic regression as well as other non-parametric methods that rely on the unimodality of the signal at and its symmetry about the target.

### 2.1.1 Impact of Signal Misspecification:

We now demonstrate the effect of parametric estimation when the signal model is misspecified and compare the results with our semiparametric estimation method developed in the next section. Three one-dimensional signal models are used for illustration. For each model,  $x_i$  is the known location of  $i$ -th sensor,  $Y_i$  is the signal strength captured by the  $i$ -th sensor,  $\theta_0$  is the unknown location of the target, and  $\epsilon_i$ 's are i.i.d noises having  $N(0, \sigma)$  distributions. We consider the interval  $[0, 5]$  for the simulation study. For each case, we estimate  $\theta_0$  based on a mis-specified parametric estimation method, and compare the results with the one-stage semiparametric estimation method proposed in the next section. The simulation results are summarized

in Table 2.1.

**Model 1:**

$$Y_i = \frac{2}{1 + \|x_i - \theta_0\|^3} + \frac{1}{(1.5 + \|x_i - \theta_0\|)^5} + \epsilon_i, \quad i = 1, 2, \dots, n$$

where  $\|\cdot\|$  is the  $L^2$  norm. We estimate  $\theta_0$  parametrically, assuming the true signal to be of the form:

$$g(\|X_i - \theta_0\|) = \frac{A}{B + \|x_i - \theta_0\|^3}$$

Note that the actual signal model is a slightly perturbed version of the model assumed in the parametric estimation method.

Next, we consider a double-exponential signal:

**Model 2:**

$$Y_i = 2e^{-\frac{\|x_i - \theta_0\|}{0.8}} + \epsilon_i, \quad i = 1, 2, \dots, n$$

We estimate  $\theta$  parametrically assuming an exponential signal: namely,

$$g(\|X_i - \theta_0\|) = Ae^{-B\|x_i - \theta_0\|^2}$$

Finally, we consider a triangular signal

Table 2.1: Comparison between misspecified parametric and semiparametric estimation

$\sigma$	n	Model 1		Model 2		Model 3	
		Parametric MSE	Semiparametric MSE	Parametric MSE	Semiparametric MSE	Parametric MSE	Semiparametric MSE
0.1	100	0.067	0.0021	0.007	0.0006	0.131	0.006
	200	0.032	0.001	0.002	0.0004	0.116	0.0016
0.3	100	0.017	0.004	0.028	0.0018	0.128	0.0022
	200	0.076	0.003	0.009	0.0007	0.110	0.0008

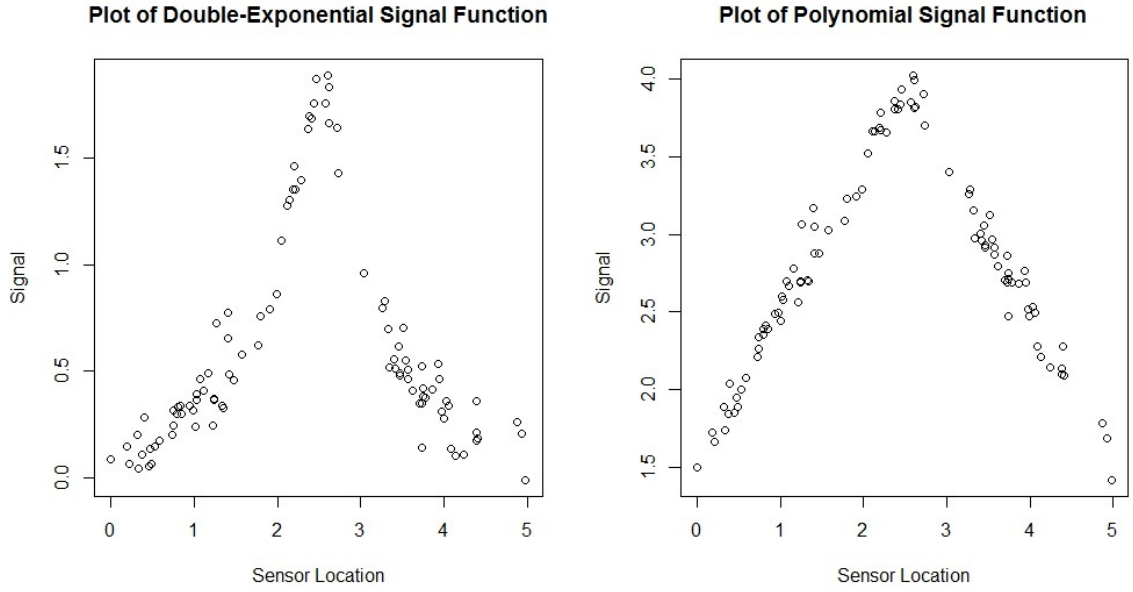


Figure 2.1: Plot of 1-dimensional Signal Functions with target at 2.5

**Model 3:**

$$Y_i = (4 - \|x_i - \theta_0\|) + \epsilon_i, \quad i = 1, 2, \dots, n$$

mis-specified by an exponential signal:

$$g(\|X_i - \theta_0\|) = Ae^{-B\|x_i - \theta_0\|^2}$$



From our summary of simulation results in Table 2.1, it is quite evident that the semiparametric method performs substantially better than the parametric estimation method with a mis-specified signal. This illustrates the risk of using a parametric estimation method, when the actual form of the signal is unknown.

## 2.2 Problem Formulation and Estimation Methods

Recall the semi-parametric model introduced in the previous section:

$Y_i = g_0(\|x_i - \theta_0\|) + \epsilon_i, i = 1, 2, \dots, n$ . Note that in the above model, the unknown target location  $\theta_0$  is the parametric component and the unknown signal function  $g_0$ , the non-parametric one. To estimate  $\theta_0$ , we propose to solve the following least squares problem:

$$\min_{g, \theta} S(\theta, g), \text{ where } S(\theta, g) = \sum_{i=1}^n (Y_i - g(\|x_i - \theta\|))^2 \quad (2.1)$$

over all monotone decreasing functions  $g$  and possible target locations  $\theta$ .

The following estimation methods are employed.

### 2.2.1 One-stage Isotonic Regression

If the target location  $\theta_0$  were known, we could have solved the minimization problem (2.1) using standard isotonic regression and find the minimizing  $g$ , say  $\hat{g}$ , which would be a step function. We adapt this idea by computing the minimizing  $g$  for every fixed  $\theta$  and then searching over  $\theta$ . This is formalized in the following algorithm:

1) Allocate  $n$  grid points uniformly within the field (taken, subsequently, to be a

square).

2) Set  $\theta$  to be each grid-point, in turn, and solve the corresponding minimization problem:

$$g_\theta = \arg \min_g S(\theta, g) \tag{2.2}$$

The above minimization problem is solved using the standard *Pool Adjacent Violators Algorithm (PAVA)* for isotonic regression (see Robertson et al. (1988)) which would provide a step function  $g_\theta$ , for all  $\theta$ . The details of this step are provided in Appendix A.

3) Store the values  $S(\theta, g_\theta)$  as  $\theta$  varies over the grid.

4) Identify, via exhaustive search,  $(\theta^*, g_{\theta^*})$  at which  $S(\theta, g_\theta)$  is at its minimum over all grid points and prescribe  $\theta^*$  as the estimate of the target.

Note that we only exploit the fact that  $g_0$  is a monotone decreasing function: the isotonic regression algorithm does not assume any particular form of  $g_0$ . Simulation results from implementations of this algorithm are presented in Section 2.4.

### 2.2.2 Two-stage Estimation Method for Target Detection

The isotonic regression method described above is computationally burdensome (and consequently time-consuming) for a large number of sensors ( $n$ ) since it involves an exhaustive search over each sensor location. Furthermore, it is not cost-effective

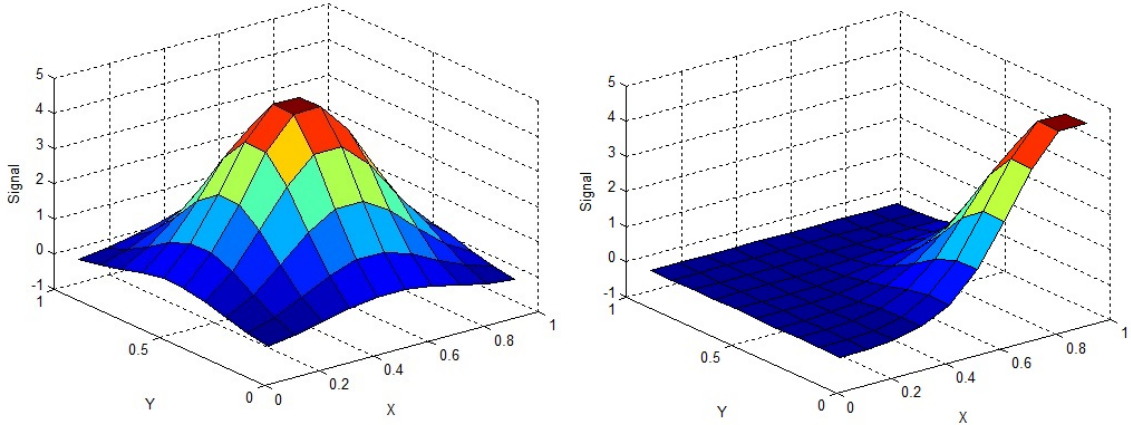


Figure 2.2: Plot of an exponential signal over unit square with target at  $(0.5, 0.5)$  and  $(0.9, 0.1)$

as it involves activating all sensors at the same time and using their recorded signals. In this section, we propose a more practical and cost-efficient adaptive two-stage method for target detection in the proposed semiparametric model, which nevertheless maintains precision. In this method, instead of activating all the  $n$  sensors at the same time, we activate  $n_1$  sensors at the first stage to detect an initial high signal region, and then activate an additional  $n_2$  sensors in the high signal region to localize the target more precisely. This method is more cost-efficient as generally, the total  $(n_1 + n_2)$  number of sensors used in this method is much smaller than  $n$ , the total number of sensors deployed in the region. The formal algorithm follows.

1. For a pilot estimate of the target location  $\theta_0 = (\theta_{10}, \theta_{20}) \in \mathbb{R}^2$ , maximize the following shorth-type criterion (Kim and Pollard (1990)):

$$\max_{\theta_1, \theta_2} \sum_{i=1}^{n_1} Y_i \mathbb{I}(\|x_{1i} - \theta_1\| \leq h_0, \|x_{2i} - \theta_2\| \leq h_0) \quad (2.3)$$

for a fixed bandwidth  $h_0$ : here,  $n_1$  represents the number of sensors used in the first stage and  $x_i = (x_{1i}, x_{2i})$  is the location of the  $i^{\text{th}}$  sensor. The symmetry and unimodal-

ity of the signal about the true  $\theta_0$  guarantees that our pilot estimate is reasonable in the sense that its precision will improve with increasing  $n_1$ . The bandwidth  $h_0$  is chosen in a way such that around 10% of the sensors in a neighborhood of  $\theta$  are captured in the above summation. The maximization is achieved via grid-search.

2. Next, use subsampling from the  $n_1$  first-stage data points and implement the above procedure to come up with an estimated target location  $\hat{\theta}^*$  for each subsample. Based on the  $\hat{\theta}^*$ 's obtained from the subsamples, construct a 95% Bonferroni confidence region (which is a rectangle) for the target location.

3. Next, identify a high signal region of the form  $\mathbb{B}(x, r)$ , which denotes a ball of radius  $r$  around point  $x \in \mathbb{R}^2$ . To this end, first define the four quadrants with respect to a point  $x$  as:

$$Q_1^x = \{(z_1, z_2) \in \mathbb{R}^2 : z_1 > x_1, z_2 > x_2\}$$

$$Q_2^x = \{(z_1, z_2) \in \mathbb{R}^2 : z_1 < x_1, z_2 > x_2\}$$

$$Q_3^x = \{(z_1, z_2) \in \mathbb{R}^2 : z_1 < x_1, z_2 < x_2\}$$

$$Q_4^x = \{(z_1, z_2) \in \mathbb{R}^2 : z_1 > x_1, z_2 < x_2\}$$

Then, fit the following piecewise constant model for the signal readings:

$$\begin{aligned} S_i &= A_1 \mathbb{I}[x_i \in \mathbb{B}(x, r)] + A_2 \mathbb{I}[x_i \in \mathbb{B}(x, r)^C \cap Q_1^x] \\ &+ A_3 \mathbb{I}[x_i \in \mathbb{B}(x, r)^C \cap Q_2^x] \\ &+ A_4 \mathbb{I}[x_i \in \mathbb{B}(x, r)^C \cap Q_3^x] \\ &+ A_5 \mathbb{I}[x_i \in \mathbb{B}(x, r)^C \cap Q_4^x], \quad i = 1, \dots, n_1 \end{aligned} \tag{2.4}$$

Search for the optimal values of  $x = (x_1, x_2)$  and  $r$  by doing a grid search in the

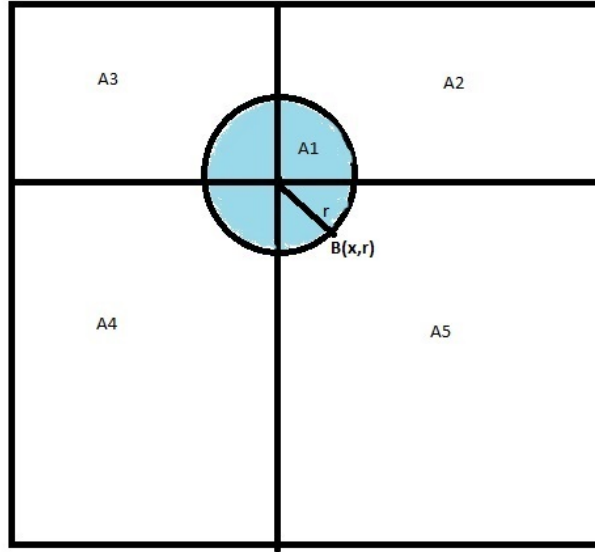


Figure 2.3: Finding high signal circular region in stage 1, using piecewise constant model

confidence region obtained from step (2) and over  $r$  such that  $\sum_{i=1}^{n_1} (Y_i - S_i)^2$  is minimized; here the optimization is performed not only over  $x$  and  $r$  but also over the  $A_i$ 's. Note that, for fixed  $x$  and  $r$ , the optimal  $A_i$ 's would be the average signal strength received by sensors in the corresponding quadrant. The corresponding optimal values  $(x^*, r^*)$  provide the high signal region  $\mathbb{B}(x^*, r^*)$  for the target location.

4. Activate  $n_2$  additional sensors, uniformly in the high signal region  $\mathbb{B}(x^*, r^*)$  and obtain the corresponding signal readings  $Y_i, i = n_1 + 1, \dots, n_1 + n_2$ . Use the readings based on  $(n_1 + n_2)$  sensors to implement the isotonic regression technique described in Section 2.2.1 and obtain the final estimate,  $\hat{\theta}_f$ , of  $\theta_0$ . The grid search required for the isotonic regression algorithm is restricted to the effective region  $\mathbb{B}(x^*, r^*)$ , in order to save time and cost. Furthermore, an adaptive grid search method that considers more grid points around the center of the ball  $\mathbb{B}(x^*, r^*)$  as compared to its edges, is used.

5. Next, obtain a bootstrap confidence region for  $\theta_0$  based on the readings from  $(n_1 + n_2)$  sensors. For each bootstrap sample, implement the isotonic regression technique described in Section 2.1 to obtain a point estimate  $\hat{\theta}^*$  and after repeating the process a considerable number of times, construct a bootstrap confidence region for  $\theta_0$ , based on the  $\hat{\theta}^*$ 's.

The method to construct the bootstrap confidence region is elaborated next.

### 2.2.3 Ellipsoidal confidence region based on Bootstrap:

Under the assumption that  $\hat{\theta}_f$  is approximately normal, we find an ellipsoidal confidence region for  $\theta_0$  in the following manner:

1. Let  $(X_1^*, Y_1^*), \dots, (X_n^*, Y_n^*)$  be a generic bootstrap sample obtained from the two-stage data and  $\hat{\theta}^*$  the corresponding estimate from Step (5) above.
2. Repeat Step (1)  $B$  times to get  $B$  bootstrap samples, and corresponding bootstrap estimates  $\hat{\theta}_1^*, \hat{\theta}_2^*, \dots, \hat{\theta}_B^*$ .
3. Compute the bootstrap estimate of the covariance matrix  $\Omega$  for  $\hat{\theta}$  as  $\hat{\Omega} = \frac{1}{B} \sum_{i=1}^B (\hat{\theta}_i^* - \bar{\theta})(\hat{\theta}_i^* - \bar{\theta})^T$ , where  $\bar{\theta} = \frac{1}{B} \sum_{i=1}^B \hat{\theta}_i^*$ .
4. Let  $C$  be the upper 95<sup>th</sup> percentile of  $\{(\hat{\theta}_i^* - \hat{\theta}_f)^T \hat{\Omega}^{-1} (\hat{\theta}_i^* - \hat{\theta}_f), i = 1, \dots, B\}$ . Then, the proposed ellipsoidal confidence region for  $\theta_0$  is:  $S = \left\{ \theta : (\theta - \hat{\theta}_f)^T \hat{\Omega}^{-1} (\theta - \hat{\theta}_f) \leq C \right\}$ .

## 2.3 Challenges with Boundary Points and a Modified Algorithm

Additional care needs to be exercised when the target is located near the boundary of the region, as the number of informative sensors is smaller compared to the case when the target is located near the center. Also, while detecting targets close to the boundary, the first-stage shorth based approach induces some bias. To circumvent these problem, we modify Step (3) of Section 2.2.2 as follows:

(3)': Instead of minimizing  $\sum_{i=1}^{n_1} (Y_i - S_i)^2$ , we minimize a weighted sum of squares:  $\sum_{i=1}^{n_1} (Y_i - S_i)^2 w_i$ , where the  $w_i$ 's are as follows: Let  $d_k^x$  be the distance of the search center  $x$  to the farthest corner point of the quadrant  $Q_k^x$ . We set  $w_i = \sum_{k=1}^4 (1/(4d_k^x))$  if  $x_i \in \mathbb{B}(x, r)$ , else  $w_i = \frac{1}{d_k^x}$ , where  $k$  is such that  $x_i \in \mathbb{B}(x, r)^C \cap Q_k^x$ .

The above recipe up-weights those quadrants where we have relatively smaller numbers of informative sensors, nullifying to an extent the effect of the bias arising from the first-stage region.

In practice, we recommend replacing Step (3) in Section 2.2.2 with Step (3)' irrespective of the true target location, since realistically we won't know whether the target is near the center or a boundary. Note that, when the target is located near the center, the weights should be similar across the different quadrants and the results should not be terribly different from the unweighted procedure, whereas for boundary points the discrepancy in the weights buys us an advantage, as already noted. In this sense, our weighting procedure is *adaptive* to the target location.

## 2.4 Performance Evaluation

The proposed estimation methods presented in Sections 2.2.1 and 2.2.2 are evaluated through an extensive simulation study. Specifically, we compare the performance of these two methods based on the *same* number of total sensor readings and show that the two-stage method gives significantly *improved target localization*. Note that in the simulation study, the same total number of sensors are used in order to establish the baseline performance of the one-stage vis-a-vis the two-stage strategy. However, the results shown in Section 2.5 indicate that statistical efficiency gains are realized even when a smaller total number of sensors is used. The results indicate that the two-stage method can attain the *same level of precision* as the one-stage method using a *smaller* budget. We demonstrate both the non-weighted (Section 2.2.2) and the modified weighted versions (Section 2.2.3) to demonstrate the effectiveness of the weighted version when the target is close to the monitoring area boundary.

The sensor field is taken to be  $[0, 5] \times [0, 5] \in \mathbb{R}^2$  and three sensor budgets: 200, 300 and 400 are considered. The noise variable  $\epsilon$  is taken to be  $N(0, \sigma)$  with  $\sigma$  assuming values from  $\sigma = 0.3, 0.5$ , which correspond to moderate and high noise levels for our models. We consider the following signal models :

1. Exponential model:  $g_0(\|x - \theta_0\|) = 2e^{-\frac{(\|x - \theta_0\|)^2}{2}}$
2. Polynomial model:  $g_0(\|x - \theta_0\|) = \frac{2}{1 + (\|x - \theta_0\|)^3}$
3. Exponential (spike) model:  $g_0(\|x - \theta_0\|) = 2e^{-\frac{(\|x - \theta_0\|)^2}{.4}}$

Two target locations are used: (2.5,2.5) in the middle of the monitored region, and (1,1) closer to the boundary. The latter location would provide insight on the perfor-



mance of the proposed framework in more challenging settings, where even methods based on parametric models exhibit subpar performance. The tabulated results given in Tables 2.2 and 2.3 are based on 300 replications for all settings considered. The performance metrics employed are: (i) the average area of the final bootstrap confidence region (CR) and (ii) the observed coverage, using percentage of times the resulting confidence region contains the true target location, at a nominal 95% level.

The obtained results clearly establish the superior performance of the two-stage procedure over its one-stage counterpart for all models and noise levels considered, both in terms of coverage and the volumes of the confidence regions, especially at smaller budgets; not only does the two-stage method provide close-to-nominal coverage, but the precision of the confidence region also improves considerably. Also, when the target is closer to the boundary, the weighted two-stage estimation method performs better than the non-weighted version (see Table 2.3) again achieving coverage nearly the nominal level. When the target is at the center, the performance of the weighted and non-weighted versions of the two-stage method are very similar (Table 2.2). We further note that the two-stage procedure is considerably less time consuming than its one-stage counterpart, as we perform the grid search only in the high signal region  $\mathbb{B}(x^*, r^*)$  for the isotonic regression step, as opposed to the one-stage method, where the grid search is done over the entire region. Based on our simulations, we observe around 30-35% reduction in the iteration time in going from the one-stage to the two-stage method.

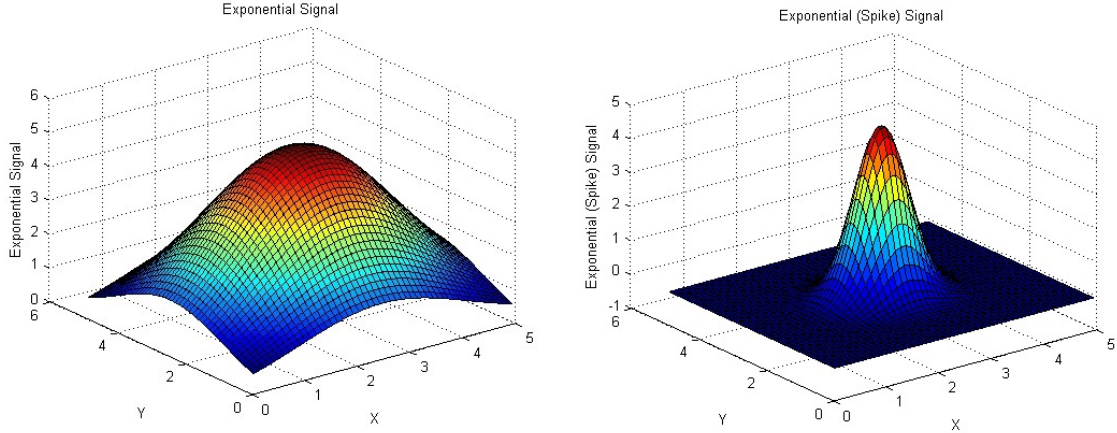


Figure 2.4: Plot of exponential signal and exponential (spike) signal with target at  $(2.5, 2.5)$

## 2.5 Applications - The ZebraNet Project

We applied the two-stage estimation method to track the movement of zebras based on data collected as part of a ZebraNet project at the Sweetwaters Game Reserve near Nanyuki, Kenya during the summer of 2005 (see Katenka et al. (2012)). The sensors were equipped with GPS location devices and were actually fitted as collars on four zebras, selected for their varying behavioral patterns. The zebras' locations and a time stamp were recorded every few minutes for approximately 10 days. In general, the ZebraNet project found that placing sensing collars on zebras did not work well, as some zebras managed to remove or lose the collars and there were other frequent hardware failures. Thus, it seems reasonable to consider a stationary sensor network for future deployments in this project instead, which would conform to the setting examined in this paper.

In order to apply the proposed algorithm in this application, the following simulated sensor experiment was designed. The original monitored region is roughly  $5\text{km} \times 5\text{km}$ ; thus, we simulated a random deployment of 400 sensors uniformly distributed

Table 2.2: 2-dim Simulation Results with target at (2.5,2.5)

$\sigma$	n	$n_1$	$n_2$	Exponential Model		
				1-stage CR avg. area(coverage)	2-stage(non-wt) CR avg.area(coverage)	2-stage(wt) CR avg. area(coverage)
0.3	200	66	134	0.110 (51%)	0.044 (94%)	0.050 (93%)
	300	100	200	0.083 (55%)	0.027 (97%)	0.031 (95%)
	400	133	267	0.054 (58%)	0.019 (97%)	0.023 (96%)
0.5	200	66	134	0.214 (79%)	0.120 (95%)	0.134 (94%)
	300	100	200	0.168 (73%)	0.078 (96%)	0.082 (94%)
	400	133	267	0.130 (84%)	0.065 (97%)	0.071 (95%)
$\sigma$	n	$n_1$	$n_2$	Polynomial Model		
				1-stage CR avg. area(coverage)	2-stage(non-wt) CR avg.area(coverage)	2-stage(wt) CR avg. area(coverage)
0.3	200	66	134	0.102 (44%)	0.027 (91%)	0.035 (92%)
	300	100	200	0.063 (53%)	0.021 (94%)	0.023 (94%)
	400	133	267	0.054 (55%)	0.015 (95%)	0.019 (93%)
0.5	200	66	134	0.265 (77%)	0.094 (97%)	0.108 (95%)
	300	100	200	0.196 (74%)	0.066 (96%)	0.074 (94%)
	400	133	267	0.110 (72%)	0.043 (97%)	0.051 (95%)
$\sigma$	n	$n_1$	$n_2$	Exponential (spike) Model		
				1-stage CR avg. area(coverage)	2-stage(non-wt) CR avg.area(coverage)	2-stage(wt) CR avg. area(coverage)
0.3	200	66	134	0.289 (66%)	0.039 (89%)	0.044 (90%)
	300	100	200	0.202 (60%)	0.015 (92%)	0.021 (91%)
	400	133	267	0.076 (62%)	0.008 (95%)	0.013 (93%)
0.5	200	66	134	0.932 (84%)	0.154 (91%)	0.172 (90%)
	300	100	200	0.572 (84%)	0.051 (97%)	0.072 (95%)
	400	133	267	0.240 (83%)	0.021 (96%)	0.027 (94%)

in the region  $[0, 5] \times [0, 5]$ , and mapped the true location of a zebra available from the ZebraNet data to this monitored region. We show the localization results for one zebra selected at random and considered its locations over a particular time period.

The emitted signals were generated according to the following model:

$$Y_i = 2e^{-\frac{(\|x_i - \theta_0\|)^2}{2}} + \epsilon_i$$

Table 2.3: 2-dim Simulation Results with target at (1,1)

$\sigma$	n	$n_1$	$n_2$	Exponential Model	
				2-stage(non-wt) CR avg. area(coverage)	2-stage(wt) CR avg.area(coverage)
0.3	200	66	134	0.14 (82%)	0.16 (90%)
	300	100	200	0.10 (86%)	0.10 (96%)
	400	133	267	0.07 (89%)	0.08 (94%)
0.5	200	66	134	0.42 (85%)	0.44 (91%)
	300	100	200	0.24 (87%)	0.26 (96%)
	400	133	267	0.20 (89%)	0.19 (95%)
$\sigma$	n	$n_1$	$n_2$	Polynomial Model	
				2-stage(non-wt) CR avg. area(coverage)	2-stage(wt) CR avg.area(coverage)
0.3	200	66	134	0.10 (73%)	0.11 (87%)
	300	100	200	0.07 (76%)	0.06 (93%)
	400	133	267	0.06 (81%)	0.05 (93%)
0.5	200	66	134	0.36 (76%)	0.34 (92%)
	300	100	200	0.18 (80%)	0.17 (96%)
	400	133	267	0.12 (83%)	0.11 (96%)
$\sigma$	n	$n_1$	$n_2$	Exponential (spike) Model	
				2-stage(non-wt) CR avg. area(coverage)	2-stage(wt) CR avg.area(coverage)
0.3	200	66	134	0.12 (80%)	0.14 (90%)
	300	100	200	0.05 (83%)	0.07 (93%)
	400	133	267	0.03 (87%)	0.04 (95%)
0.5	200	66	134	0.52 (83%)	0.50 (91%)
	300	100	200	0.18 (86%)	0.16 (94%)
	400	133	267	0.07 (90%)	0.08 (96%)

where  $\epsilon_i \sim N(0, \sigma)$  with  $\sigma = 0.5$  to simulate noisy signal readings. We then applied our two-stage method to find a confidence region for the location of the zebra, over a particular time period. Initially, we activated 100 sensors at random, and determined the high signal region  $\mathbb{B}(x^*, r^*)$  as in Step (3)' of the two-stage method. Next, we activated the remaining sensors in  $\mathbb{B}(x^*, r^*)$ , i.e. the ones that had not been picked at the first stage, to obtain our second stage data. We considered six different time points (corresponding to six different target locations). The locations of the selected zebra over the entire study period are depicted in Figure 2.5 and those at the six cho-

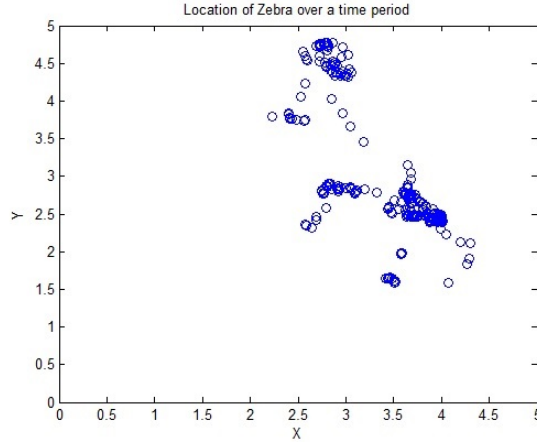


Figure 2.5: Locations of the zebra in study period

sen time points and their corresponding estimated confidence regions in Figure 2.6, where the ellipsoidal grey region is the estimated confidence region and the black dot inside corresponds to the true location. From our analysis, we note that the two-stage method shows satisfactory performance, producing fairly precise confidence regions. Also, the total number of sensors used by the method is much smaller than 400, which makes the method cost-efficient.

In order to evaluate the performance of the one-stage method in this set-up, we also activated 200 sensors at random and implemented the one-stage estimation procedure to construct bootstrap confidence regions for the location of the zebra. Table 2.4 reports the co-ordinates of the zebra at the selected time points, the areas of corresponding one-stage confidence regions, the areas of the corresponding two-stage confidence regions and the number of sensors activated at the second stage. Even though we, typically, use far less than 200 sensors in total for the two-stage procedure, we obtain more precise confidence regions compared to those obtained by the one-stage method, establishing its effectiveness and cost-efficiency.

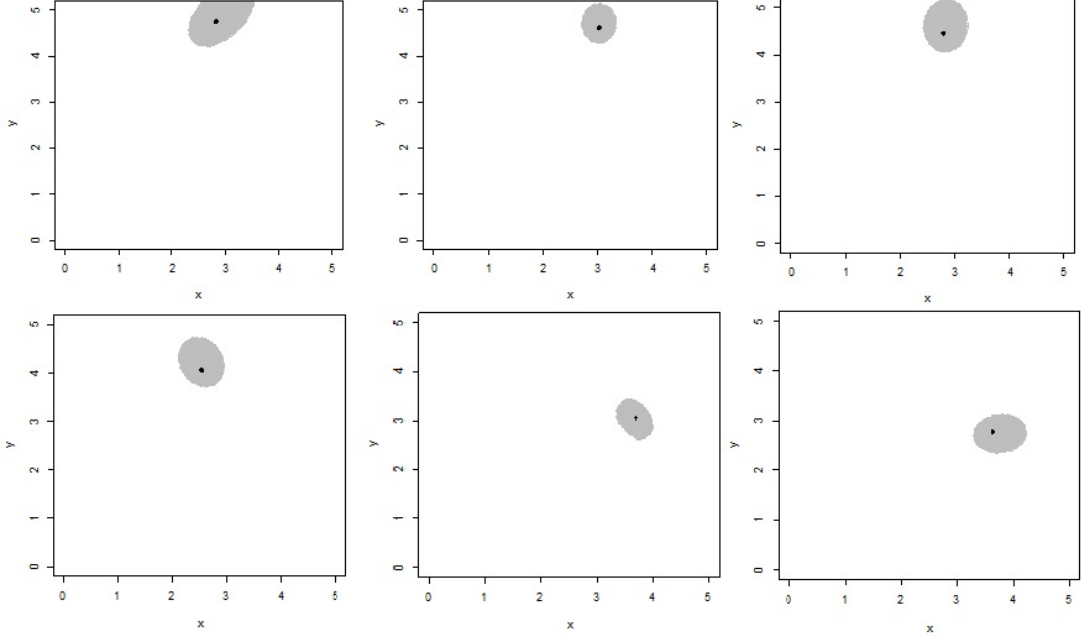


Figure 2.6: Two-Stage Confidence Region of zebra location at six time points based on Exponential Signal

### 2.5.1 Robustness to Model Misspecification

We have, thus far, considered *isotropic* signal models, where the signal strength received by sensor  $x_i$  depends only on the distance between  $x_i$  and the target location  $\theta_0$ , i.e., the contours of the signal are circles around the target. We now demonstrate that the proposed method is fairly robust to minor deviations from isotropy using the Zebranet data. Assume the following *anisotropic* signal model:

$$Y_i = 2e^{-\left(\frac{\|x_{1i}-\theta_{10}\|^2}{2} + \frac{\|x_{2i}-\theta_{20}\|^2}{3}\right)} + \epsilon_i$$

where  $\epsilon_i \sim N(0, \sigma)$ ,  $x_i = (x_{1i}, x_{2i}) \in \mathbb{R}^2$ ,  $\theta_0 = (\theta_{10}, \theta_{20})$  is the target location.

As before, we detect the location of the zebra at different time points by constructing a confidence region using the two-stage estimation method. The true locations of the zebra at six chosen time points and the corresponding estimated confidence regions are shown in Figure 2.7, where the black dot inside the grey ellipsoidal confidence region corresponds to the true location of the zebra. It can be seen that our method continues

Table 2.4: Performance of One-stage and Two-stage methods at zebra tracking, based on Exponential Signal

Zebra Location	Area of One-Stage CR	Area of Two-Stage CR	No. of sensors used at second stage
(2.82, 4.74)	1.15	0.90	37
(3.02, 4.61)	1.04	0.36	33
(2.80, 4.46)	2.52	0.62	37
(2.53, 4.06)	0.74	0.57	65
(3.68, 3.05)	0.47	0.34	69
(3.63, 2.78)	0.65	0.50	96

to perform satisfactorily in this setting, further demonstrating the robustness of the proposed modeling framework. A detailed investigation of methods that adapt to potential anisotropy will be discussed in Chapter III.

## 2.6 Theoretical Issues

While the methodology presented in this chapter is attractive from several perspectives, a theoretical analysis of these procedures is unavailable at this point and will be the topic of future research. Our model is a special case of the ‘bundled parameters’ problem – the nuisance parameter  $g_0$  contains the parameter of interest  $\theta_0$  as part of its argument – which is well-known to be notoriously difficult, especially without using smoothing techniques for estimating the  $g_0$  function. On the other hand, a major methodological advantage of our approach is the use of isotonic regression which does not require a smoothing parameter thereby simplifying the implementation of our procedure considerably. Kernel or spline based procedures, though theoretically more tractable, have to deal with a tuning parameter, practical choices for which can often be tricky (Heidenreich et al. (2013)).

The difficulty of studying least squares/maximum likelihood methods in the bundled parameters problem is exemplified by the work of Murphy et. al. (1999) who studied maximum likelihood type estimates of the slope parameters in a linear re-

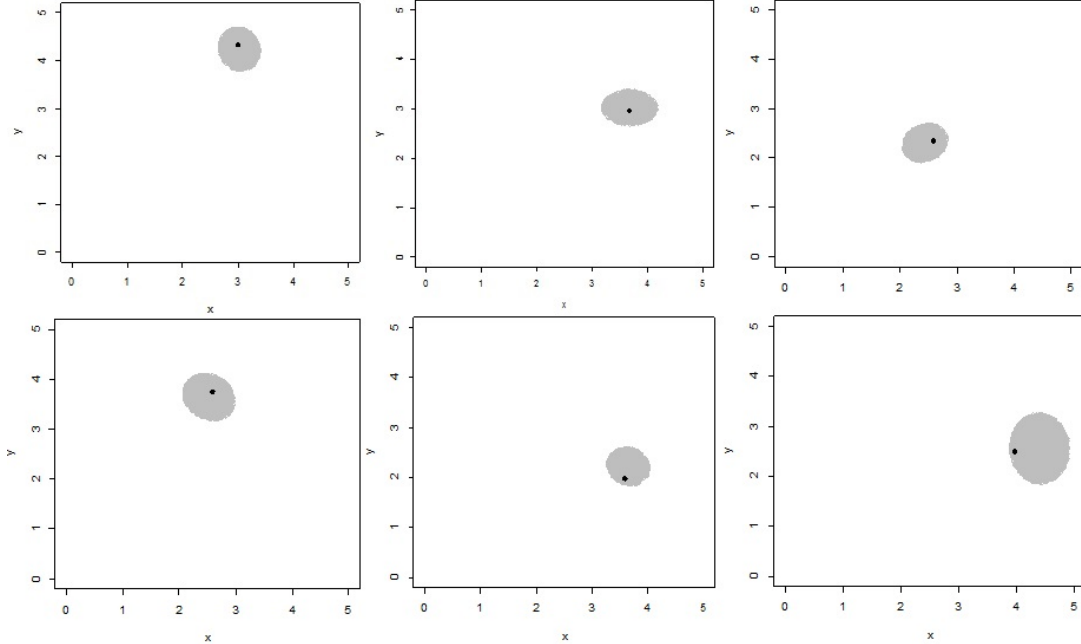


Figure 2.7: Two-Stage Confidence Region of zebra location at six time points, based on Anisotropic Signal

gression model under current status censoring on the response. In that paper, a cube-root convergence rate is obtained for the slope estimate, but what remains unclear is whether this rate is sub-optimal. To the best of our knowledge, there has been no work thus far on semiparametric models with bundled parameters where the finite-dimensional parameter (the target location in our setting) has been shown to be estimable at the parametric  $\sqrt{n}$  rate by its non-regularized MLE/least squares estimate, let alone shown to be asymptotically normal. On the other hand,  $\sqrt{n}$ -consistency can be established, with significant effort, by taking recourse to some form of smoothing, demonstrated for example in Ding and Nan (2012) who employ a B-spline based estimation procedure for the non-parametric component in censored linear regression models of the type considered in Murphy et. al. (1999). The single-index model is another famous bundled-parameters model that has a long history in econometrics, but has again been traditionally studied through smooth approximations for the non-parametric component: see, for example, Hall (1989), Powell, Stock



and Stoker (1989), Ichimura (1993), Härdle, Hall and Ichimura (1993), Horowitz and Härdle (1996), Wang and Yang (2009). In their paper on semiparametric bundled parameter estimation, Ichimura and Lee (2010) have shown, more generally, that under appropriate conditions, the asymptotic distribution of the parametric component would be normal when the nonparametric component is estimated by a smooth function. Theoretical results for a smoothed version of the current procedure can possibly be obtained using the results of their paper and will be a topic of future study.

As far as our non-smooth procedure is concerned, there is preliminary empirical evidence that the one-stage isotonic estimate of  $\theta_0$  has the  $\sqrt{n}$  convergence rate, as well as an asymptotic normal distribution in the one-dimensional problem. The relevant plots and figures are provided in Appendix B. Our elliptical confidence regions show good empirical performance: while asymptotic normality would certainly be a sufficient explanation for this, it may not be necessary for the observed good behavior of the elliptical regions. In any case, it is amply clear that the development of the methodology opens up a number of avenues for deep theoretical investigation.

## CHAPTER III

# Target Estimation Based on Anisotropic Signal

### 3.1 Introduction

In chapter II, we proposed target estimation methods for semiparametric isotropic signal models, where the signal decays uniformly in each direction from the target location, producing circular contours of sensor locations where the signal strengths received are similar. In these models, the signal strength captured by a sensor depends only on the distance of the sensor from the target and is independent of the direction in which the sensor is located from the target. However, in many practical scenarios, that may not be the case. In many real life scenarios, the signal may decay at different rates in different directions and is no longer isotropic. The methods discussed in chapter II may perform poorly in those cases because they depend heavily on the isotropic nature of the signal and do not take into account the directional variation in the signal propagation, if there is any. In this chapter, we address the problem of target estimation for anisotropic signal and propose a clustering based method for anisotropic signals where the signal contours are ellipsoidal in nature.

For anisotropic signal models with ellipsoidal contours, the captured signal strengths can be modeled as:  $Y_i = g_0 \left( (x_i - \theta_0)^T \Sigma^{-1} (x_i - \theta_0) \right) + \epsilon_i, i = 1, 2, \dots, N$ , where  $x_i \in \mathbb{R}^2$  is the known location of the  $i$ -th sensor,  $\theta_0$  is the unknown location of the

target,  $\Sigma$  is an unknown symmetric matrix which controls the shape and alignment of the ellipsoidal contours and  $g_0$  is an unknown monotone decreasing function. As before, our primary goal is to estimate  $\theta_0$ , the true location of the target present. In this chapter, we develop a clustering based algorithm to efficiently detect the location of the target when the signal model is anisotropic in nature and also construct relevant confidence regions. The performance of the proposed method is demonstrated through simulation results and real data applications. A major advantage of our approach is that we do not have to estimate the signal function  $g_0$  in this case, which can be tricky specially for anisotropic signal models.

The isotonic estimation method, though robust to minor deviations from isotropy as shown in chapter II, may perform poorly at substantial levels of anisotropy which we illustrate through simulations. The sensor field is taken to be  $[0, 5] \times [0, 5] \in \mathbb{R}^2$  and two sensor budgets: 300 and 400 are considered. The noise variable  $\epsilon$  is taken to be  $N(0, \sigma)$  with  $\sigma = 0.1$ . We consider the following anisotropic signal models  $g_0$ , with target located at  $(2.5, 2.5)$ :

1. Exponential model:  $g_0 \left( (x_i - \theta_0)^T \Sigma^{-1} (x_i - \theta_0) \right) = 2e^{-(x_i - \theta_0)^T \Sigma^{-1} (x_i - \theta_0)}$
2. Polynomial model:  $g_0 \left( (x_i - \theta_0)^T \Sigma^{-1} (x_i - \theta_0) \right) = \frac{2}{1 + ((x_i - \theta_0)^T \Sigma^{-1} (x_i - \theta_0))^{3/2}}$
3. Exponential (spike) model:  $g_0 \left( (x_i - \theta_0)^T \Sigma^{-1} (x_i - \theta_0) \right) = 4e^{-((x_i - \theta_0)^T \Sigma^{-1} (x_i - \theta_0))^{\frac{1}{2}}}$

In above study, we use  $\Sigma = \begin{pmatrix} 1 & \rho \\ \rho & 1 \end{pmatrix}$  with  $\rho = 0.5, 0.8$ .

The ellipsoidal contours formed by sensors receiving similar signal strengths for the polynomial model are illustrated in Figure 3.1. We use the Isotonic estimation method for target detection described in Chapter II and obtain average area of resulting con-

confidence regions and the observed coverage percentages. The results are provided in Table 3.1. Clearly, the Isotonic method performs poorly for the above anisotropic signal models. Later in section 3.3 , we apply the clustering based method proposed in this Chapter to the above anisotropic models and show that it produces confidence regions with better coverages, as illustrated in Table 3.2.

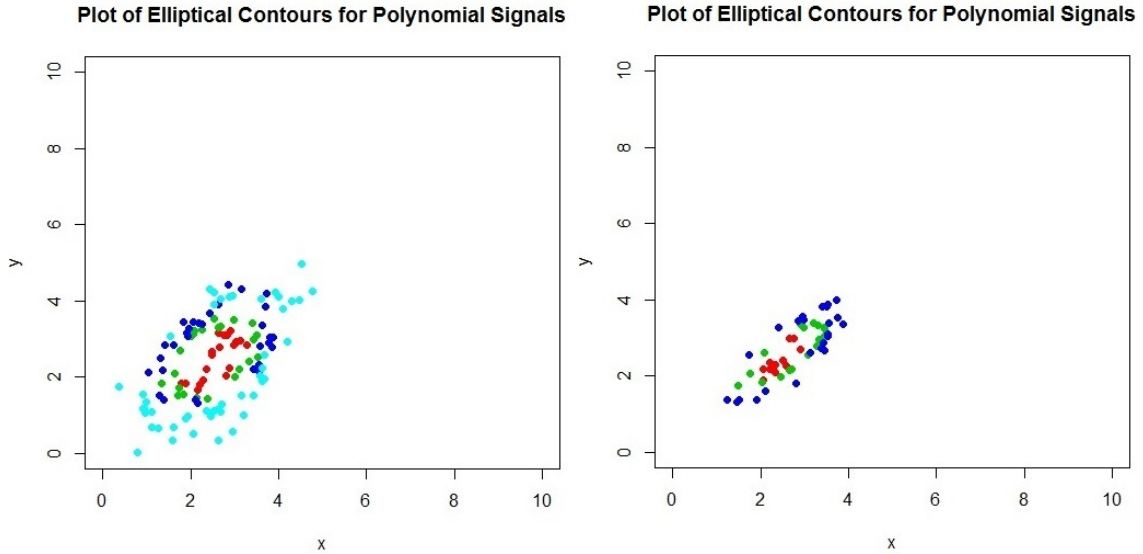


Figure 3.1: Plot of Ellipsoidal Contours formed by Sensors for Polynomial Signal Model with  $\rho = 0.5, 0.8$

Table 3.1: Simulation Results for Anisotropic Models with target at (2.5,2.5), Using Isotonic Estimation Method

$\sigma$	$\rho$	n	Exponential Model avg. area(coverage)	Polynomial Model avg.area(coverage)	Exponential (Spike) Model avg. area(coverage)
0.1	0.5	300	0.053 (54%)	0.060 (53%)	0.044 (45%)
		400	0.032 (64%)	0.043 (56%)	0.028 (50%)
0.1	0.8	300	0.063 (42%)	0.066 (50%)	0.054 (65%)
		400	0.047 (45%)	0.060 (56%)	0.046 (75%)

## 3.2 Problem Formulation and Estimation Methods

Recall the semi-parametric model introduced in the previous section:

$Y_i = g_0 \left( (x_i - \theta_0)^T \Sigma^{-1} (x_i - \theta_0) \right) + \epsilon_i, i = 1, 2, \dots, n.$  Note that in the above model, the unknown target location  $\theta_0$  is the parametric component and the unknown signal function  $g_0$ , the non-parametric one. In the above anisotropic signal model, the propagating signal has an elliptical contour, i.e., the sensors capturing similar signal strengths should lie on an ellipsoidal region. The unknown symmetric matrix  $\Sigma$  controls the shape and alignment of the ellipsoidal contours.

Note that in the above signal model, the sensors receiving similar signal strengths should lie on an ellipse of the form  $(x_i - \theta_0)^T \Sigma^{-1} (x_i - \theta_0) = C$ , with the center of the ellipse at  $\theta_0$ , where  $C$  is some constant. Also, the sensors capturing high signal strengths are expected to be located close to the true target location, hence the corresponding ellipse should be close to the target location with a small value of the constant  $C$ . As we move further away from the target, the corresponding ellipses would be more spread out and have high values for constant  $C$ . Together, all these ellipses would form a concentric family of ellipses with the center being the true target location  $\theta_0$ . Also, the ellipses near the center should have relatively low noise due to high signal strengths, whereas the ellipses further away from the centers are expected to have significant noise in the signal strengths captured by the corresponding sensors. This phenomenon is illustrated in Figure 3.2, where sensors receiving similar signal strengths form ellipsoidal contours with the center being the true target location  $\theta_0$ . We exploit the above geometric property of the anisotropic signal model and propose the following clustering based estimation method for estimating target location  $\theta_0$ :

1. First, we implement the k-means clustering method to cluster the observed

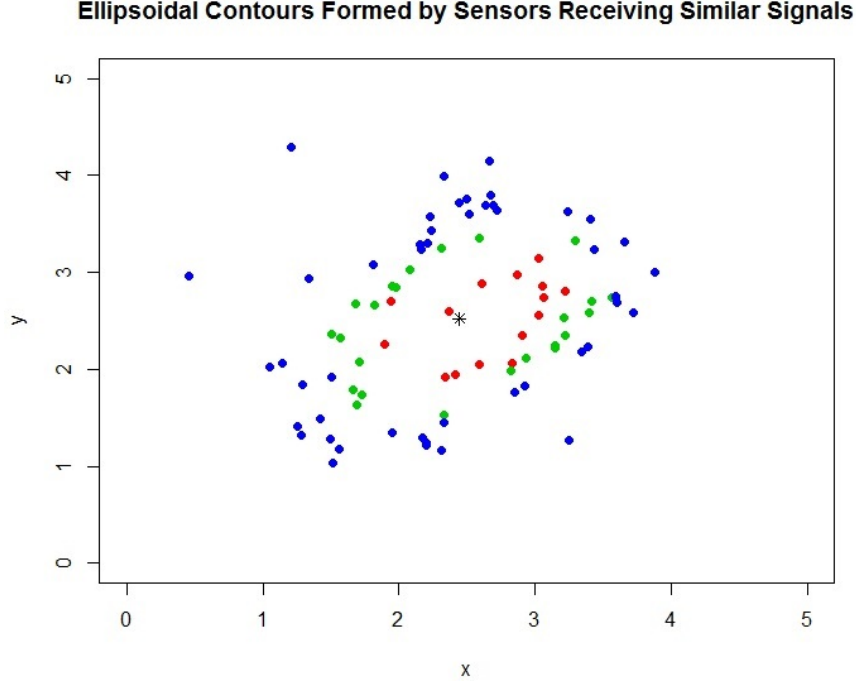


Figure 3.2: Ellipsoidal Contours Formed by Sensors Receiving Similar Signals, obtained by Clustering, with Target at (2.5, 2.5)

signal readings  $Y_i$ 's. We use the following well known "Elbow" method (Thorndike, 1953) to choose optimal number of clusters: we consider the ratio  $B(k)/TSS$  as a function of no. of clusters  $k$ , where  $B(k)$  and  $TSS$  are the *between-cluster sum of squares* and *total sum of squares* of signal readings  $Y_i$ 's with  $k$  clusters. To be more specific, for signal readings  $Y_1, \dots, Y_n$  clustered in  $k$  groups,

$$B(k) = \sum_{i=1}^k |C_i| (\bar{Y}_i - \bar{Y})^2 \text{ and } TSS = \sum_{i=1}^n (Y_i - \bar{Y})^2$$

where  $\bar{Y} = \sum_{i=1}^n Y_i/n$ ,  $\bar{Y}_i = \sum_{j \in C_i} Y_j/|C_i|$ , and  $C_i$  denotes the  $i^{th}$  cluster.

If we plot the ratio  $B(k)/TSS$  as a function of  $k$ , the first few clusters will provide considerable information (in terms of explaining the variance in the data), but at some point the marginal gain will become negligible, giving an angle in the graph. We capture this "elbow" point by fitting a kink model of  $B(k)/TSS$  over  $k$  and get the desired number of clusters. More specifically, we regress  $B(k)/TSS$  over  $k$ , splitting the range of  $k$  in two different parts such that we get two best fitting lines for part 1

and part 2, in terms of minimizing the overall error sum of squares, and choose the minimizing value of  $k$  as the desired number of clusters. The method is illustrated below:

Let,  $P_1^j = \{(2, B(2)/TSS), \dots, (j, B(j)/TSS)\}$  and

$P_2^j = \{(j + 1, B(j + 1)/TSS), \dots, (K, B(K)/TSS)\}$ ,

where  $K$  is the maximum number of clusters considered. Next we linearly regress the points in  $P_1^j$  and  $P_2^j$  to get two least squares lines and let  $G_j$  denote the total error sum of squares obtained by fitting those two lines. Let  $k^* = \arg \min_j G_j$ , then we choose  $k^*$  as the optimal number of clusters.

As an alternative, one can also fit the following "Broken Stick" model:

$$Y = \beta_0 + \beta_1 X + \beta_2 (X - C)^+ + \epsilon,$$

with  $B(k)/TSS$  as the  $Y$  variable and  $k$  as the  $X$  variable and search for the optimal change point  $C$  which provides the best fit. That optimal change point  $C$  would provide the number of informative clusters for our problem.

Our simulations have shown that both methods perform similarly in identifying the number of informative clusters. This method is illustrated in Figure 3.3, where the red circle denotes the "elbow" point.

2. Next, for each cluster, we consider the corresponding sensor locations  $x_i$ 's and fit an ellipse through them, using least square ellipse fitting method. More specifically, let  $(x_{11}, x_{21}), \dots, (x_{1n_i}, x_{2n_i})$  be the corresponding sensor locations for the  $i^{th}$  cluster, with  $|C_i| = n_i$ . An ellipse can be described by the following implicit second order

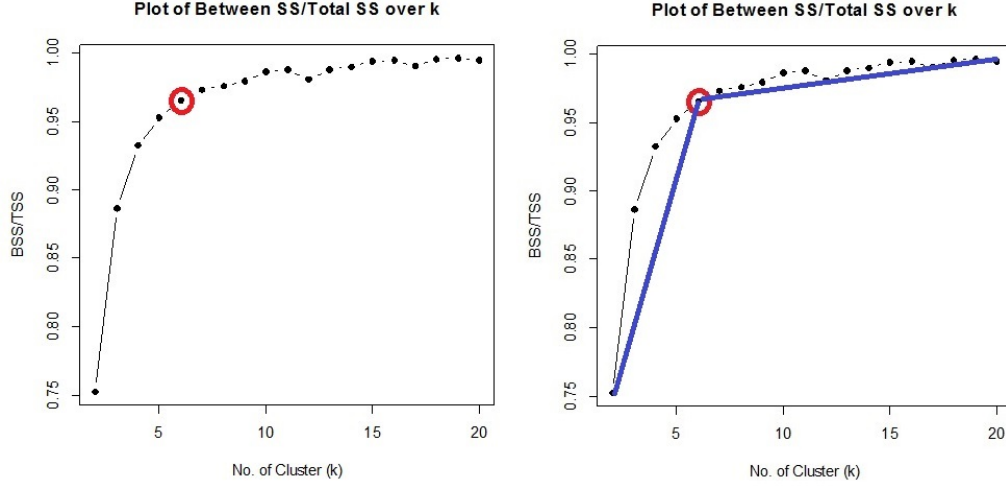


Figure 3.3: Plot of  $B(k)/TSS$  over  $k$  and the "elbow" point

polynomial:

$$F(x, y) = ax^2 + bxy + cy^2 + dx + ey + f = 0$$

with an ellipse specific constraint  $b^2 - 4ac < 0$ .

Let  $\alpha = [a, b, c, d, e, f]^T$ . Then, we can fit an ellipse through the sensor locations  $(x_{11}, x_{21}), \dots, (x_{1n_i}, x_{2n_i})$  by minimizing the sum of squared algebraic distances of the points to the ellipse:  $\min_{\alpha} \sum_{j=1}^{n_i} F(x_{1j}, x_{2j})^2$  with the constraint  $b^2 - 4ac < 0$  (see Fitzgibbon et al.(1999)).

Thus, if we have  $k$  clusters, we fit  $k$  ellipses based on the sensor locations corresponding to each cluster.

3. In order to get a measure of goodness of fit for the fitted ellipses, we calculate the following sum of squares measure for each cluster  $j$ :

$$SSE_j = \sum_{i \in C_j} d^2(x_i, E_j) / |C_j|$$



where cluster  $C_j$  consists of the the sensor locations  $x_i$ 's which belong to  $j^{th}$  cluster, and  $d(x_i, E_j)$  denotes the algebraic distance between the sensor location  $x_i$  and the fitted ellipse  $E_j$  for cluster  $C_j$ . Also,  $|C_j|$  denotes the number of points in cluster  $C_j$ .

4. Next, in order to identify the informative clusters and eliminate the noisy ones, we fit a "stump" model based on the data:  $\{(j, SSE_j) : j = 1, \dots, k\}$ .

Specifically, we try to minimize the following criterion:

$$\min_{u,A,B} \sum_{j \in \{C_1, \dots, C_u\}} (SSE_j - A)^2 + \sum_{j \in \{C_{u+1}, \dots, C_k\}} (SSE_j - B)^2 \quad (3.1)$$

over  $u$ ,  $A$  and  $B$ . where  $C_1, \dots, C_k$  are the clusters of signal readings  $Y_i$ 's, arranged in decreasing order of the cluster means. So, the sensors corresponding to cluster  $C_1$  are expected to be closest to the target location, whereas the sensors corresponding to cluster  $C_k$  are expected to be the farthest. Let  $u^*$  be the optimal value of  $u$  which minimizes (3.1). The method is illustrated in Figure 3.4, where  $u^*$  is 3.

5. Finally, we consider only the fitted ellipses  $E_1, \dots, E_{u^*}$  and consider their centers. We propose the following methods to compute the final estimate of  $\theta_0$ :

**Method 1 (Unweighted Mean):** Compute the mean of the centers of ellipses  $E_1, \dots, E_{u^*}$  and take that as the final estimate  $\hat{\theta}_f$  of  $\theta_0$ .

**Method 2 (Weighted Mean):** Compute a *weighted* mean of centers of ellipses  $E_1, \dots, E_{u^*}$  with weights  $w_i \propto \frac{1}{SSE_i}$  and take the weighted mean as the final estimate  $\hat{\theta}_f$  of  $\theta_0$ .

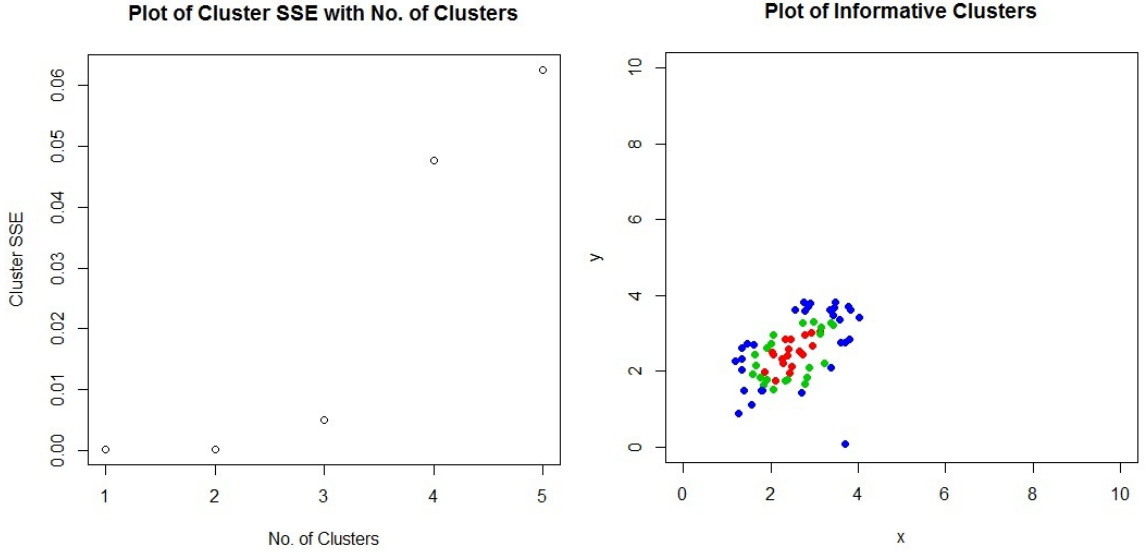


Figure 3.4: Finding No. of Informative Clusters with target at  $(2.5, 2.5)$

6. Finally, we obtain a subsampling based confidence region for  $\theta_0$  based on the readings from sensors. For each subsample, implement the estimation technique described above to obtain a point estimate  $\hat{\theta}^*$  and after repeating the process a considerable number of times, construct a confidence region for  $\theta_0$ , based on the  $\hat{\theta}^*$ 's.

The method to construct the subsampling based confidence region, is elaborated next.

### 3.2.1 Ellipsoidal confidence region based on Subsampling:

Under the assumption that  $\hat{\theta}_f$  is approximately normal, we find an ellipsoidal confidence region for  $\theta_0$  in the following manner:

1. Let  $(X_1^*, Y_1^*), \dots, (X_{n^*}^*, Y_{n^*}^*)$  be a generic sub-sample obtained from the data and  $\hat{\theta}^*$  the corresponding estimate from Step (5) above. We consider the sample size for sub-sampling to be 70% of the original sample size.
2. Repeat step (1)  $B$  times to get  $B$  sub-samples, and corresponding estimates

$$\hat{\theta}_1^*, \hat{\theta}_2^*, \dots, \hat{\theta}_B^*.$$

3. Compute the sub-sample estimate of the covariance matrix  $\Omega$  for  $\hat{\theta}$  as  $\hat{\Omega} = \frac{1}{B} \sum_{i=1}^B (\hat{\theta}_i^* - \bar{\theta})(\hat{\theta}_i^* - \bar{\theta})^T$ , where  $\bar{\theta} = \frac{1}{B} \sum_{i=1}^B \hat{\theta}_i^*$ .

4. Let  $C$  be the upper 95<sup>th</sup> percentile of the quantities  $\{(\hat{\theta}_i^* - \hat{\theta}_f)^T \hat{\Omega}^{-1} (\hat{\theta}_i^* - \hat{\theta}_f), i = 1, \dots, B\}$ . Then, the proposed ellipsoidal confidence region for  $\theta_0$  is:

$$S = \left\{ \theta : (\theta - \hat{\theta}_f)^T \hat{\Omega}^{-1} (\theta - \hat{\theta}_f) \leq C \right\}.$$

### 3.3 Performance Evaluation

In this section, we evaluate the performance of the proposed estimation methods in Sections 3.2 and 3.2.1 using simulations, where we evaluate the performances the proposed methods for three different signal models.

The sensor field is taken to be  $[0, 5] \times [0, 5] \in \mathbb{R}^2$  and three sensor budgets: 200, 300 and 400 are considered. The noise variable  $\epsilon$  is taken to be  $N(0, \sigma)$  with  $\sigma$  assuming values from  $\sigma = 0.1, 0.2$ , which correspond to moderate and high noise levels for our models. We consider the following signal models  $g_0$ :

1. Exponential model:  $g_0 \left( (x_i - \theta_0)^T \Sigma^{-1} (x_i - \theta_0) \right) = 2e^{-(x_i - \theta_0)^T \Sigma^{-1} (x_i - \theta_0)}$
2. Polynomial model:  $g_0 \left( (x_i - \theta_0)^T \Sigma^{-1} (x_i - \theta_0) \right) = \frac{2}{1 + ((x_i - \theta_0)^T \Sigma^{-1} (x_i - \theta_0))^{3/2}}$
3. Exponential (spike) model:  $g_0 \left( (x_i - \theta_0)^T \Sigma^{-1} (x_i - \theta_0) \right) = 4e^{-((x_i - \theta_0)^T \Sigma^{-1} (x_i - \theta_0))^{\frac{1}{2}}}$

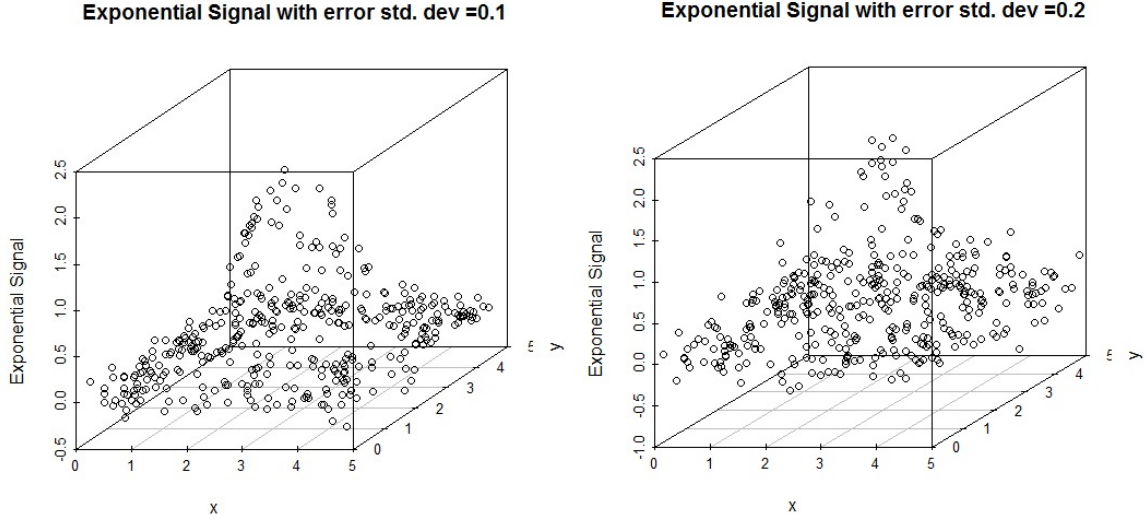


Figure 3.5: Plot of Exponential Signals with Different Noise Levels

Two target locations are used:  $(2.5, 2.5)$  at the middle of the region, and  $(1, 1)$  closer to the boundary. As before, the latter location would provide insight on the performance of the proposed framework in more challenging settings, where even methods based on parametric models exhibit subpar performance. Also we apply both Method 1 (Unweighted Mean) and Method 2 (Weighted Mean) as discussed in step (5) of the algorithm and compare their performances. The tabulated results given in Tables 3.2 and 3.3 are based on 300 replications for all settings considered. The performance metrics employed are: (i) the average area of the final sub-sample confidence region (CR) and (ii) the observed coverage, using percentage of times the resulting confidence region contains the true target location, at a nominal 95% level. The plots of Exponential and Exponential (spike) signals with target at  $(2.5, 2.5)$  and  $(1, 1)$  are provided in Figures 3.6 and 3.7.

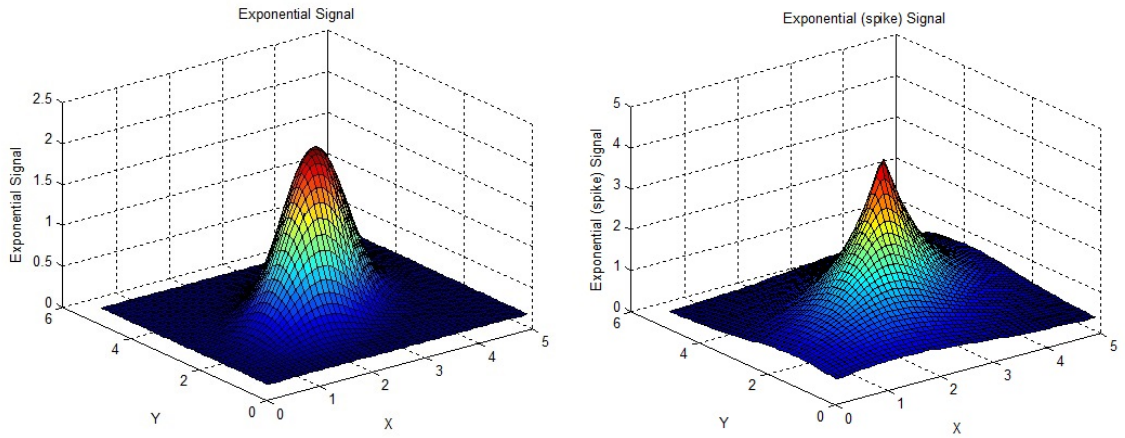


Figure 3.6: Plot of Exponential and Exponential(spike) signals for target at (2.5, 2.5)

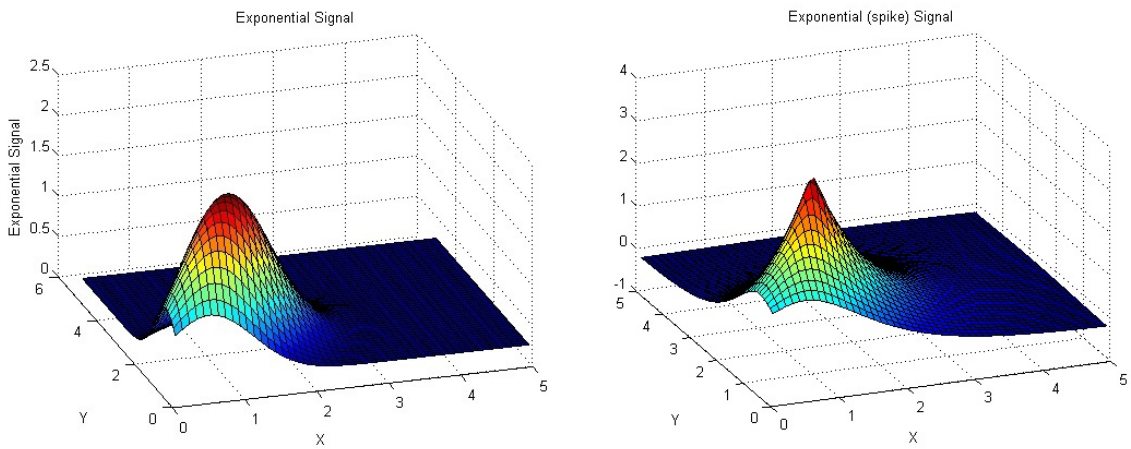


Figure 3.7: Plot of Exponential and Exponential(spike) signals for target at (1, 1)

In our simulation study, we use  $\Sigma = \begin{pmatrix} 1 & \rho \\ \rho & 1 \end{pmatrix}$  with  $\rho = 0.5, 0.8$ .

The configuration of the ellipsoidal contours of the signal model depends on  $\rho$ . High values of  $\rho$  would correspond to high correlation between the  $x$  and  $y$  coordinates and would shrink the ellipse further. The obtained simulation results (demonstrated in Tables 3.2 and 3.3) clearly establish quite accurate performance of the proposed methods for all models and noise levels considered, both in terms of coverage and the volumes of the confidence regions. Method 1 and Method 2 perform quite similarly for the target location  $(2.5, 2.5)$ ; however, for high noise scenarios with the target at  $(1,1)$ , Method 2 provides more accurate confidence regions than Method 1. Comparing the performances of the proposed methods for two locations  $(2.5, 2.5)$  and  $(1, 1)$ , we see that, on average, the areas of the corresponding confidence regions are higher for the boundary point  $(1, 1)$ , which is expected as detecting the location accurately near the boundary is more challenging due to the presence of a smaller number of informative sensors. Also, as expected, the confidence regions become more precise as the number of sensors increases and noise level decreases. Some examples of the informative ellipses formed by the sensors with  $\rho = 0.5, 0.8$  are provided in Figures 3.8 and 3.9.

### 3.3.1 Comparison with Isotonic Regression Method

Recall that in Chapter II, we developed an isotonic regression based method to estimate the target location for isotropic signal model. We can also apply the clustering based method proposed in this chapter for isotropic model and see how it performs compared to the isotonic regression method. Once again, we consider the following

Table 3.2: 2-dim Simulation Results with target at (2.5,2.5)

$\sigma$	$\rho$	n	Exponential Model	
			Method 1 (Unweighted Mean) avg. area(coverage)	Method 2 (Weighted Mean) avg.area(coverage)
0.1	0.5	200	0.111 (97%)	0.177 (97%)
		300	0.058 (98%)	0.100 (96%)
		400	0.040 (97%)	0.042 (97%)
0.1	0.8	200	0.243 (96%)	0.261 (97%)
		300	0.144 (97%)	0.120 (94%)
		400	0.087 (96%)	0.070 (95%)
0.2	0.5	200	0.272 (95%)	0.195 (94%)
		300	0.174 (97%)	0.120 (96%)
		400	0.134 (98%)	0.074 (95%)
0.2	0.8	200	0.465 (95%)	0.232 (96%)
		300	0.385 (96%)	0.125 (95%)
		400	0.306 (93%)	0.085 (94%)
$\sigma$	$\rho$	n	Polynomial Model	
			Method 1 (Unweighted Mean) avg. area(coverage)	Method 2 (Weighted Mean) avg.area(coverage)
0.1	0.5	200	0.055 (97%)	0.074 (97%)
		300	0.026 (96%)	0.050 (95%)
		400	0.016 (97%)	0.025 (95%)
0.1	0.8	200	0.095 (96%)	0.126 (97%)
		300	0.039 (97%)	0.070 (95%)
		400	0.025 (95%)	0.048 (97%)
0.2	0.5	200	0.163 (93%)	0.166 (94%)
		300	0.085 (94%)	0.090 (96%)
		400	0.063 (96%)	0.061 (94%)
0.2	0.8	200	0.294 (95%)	0.247 (95%)
		300	0.206 (96%)	0.126 (97%)
		400	0.140 (97%)	0.074 (94%)
$\sigma$	$\rho$	n	Exponential (Spike) Model	
			Method 1 (Unweighted Mean) avg. area(coverage)	Method 2 (Weighted Mean) avg.area(coverage)
0.1	0.5	200	0.034 (96%)	0.053 (96%)
		300	0.021 (95%)	0.041 (96%)
		400	0.014 (96%)	0.027 (97%)
0.1	0.8	200	0.053 (95%)	0.077 (96%)
		300	0.022 (96%)	0.042 (93%)
		400	0.015 (94%)	0.029 (95%)
0.2	0.5	200	0.070 (95%)	0.082 (96%)
		300	0.043 (96%)	0.061 (97%)
		400	0.028 (97%)	0.043 (97%)
0.2	0.8	200	0.095 (95%)	0.124 (97%)
		300	0.057 (95%)	0.073 (93%)
		400	0.041 (94%)	0.062 (96%)

Table 3.3: 2-dim Simulation Results with target at (1,1)

$\sigma$	$\rho$	n	Exponential Model	
			Method 1 (Unweighted Mean) avg. area(coverage)	Method 2 (Weighted Mean) avg.area(coverage)
0.1	0.5	200	0.537 (96%)	0.547 (97%)
		300	0.167 (97%)	0.120 (96%)
		400	0.057 (94%)	0.067 (96%)
0.1	0.8	200	0.978 (97%)	0.408 (97%)
		300	0.348 (95%)	0.158 (94%)
		400	0.098 (96%)	0.087 (96%)
0.2	0.5	200	1.536 (94%)	0.530 (95%)
		300	0.940 (95%)	0.304 (97%)
		400	0.894 (90%)	0.177 (95%)
0.2	0.8	200	1.880 (89%)	0.365 (93%)
		300	1.575 (93%)	0.166 (94%)
		400	1.103 (98%)	0.158 (95%)
$\sigma$	$\rho$	n	Polynomial Model	
			Method 1 (Unweighted Mean) avg. area(coverage)	Method 2 (Weighted Mean) avg.area(coverage)
0.1	0.5	200	0.429 (94%)	0.542 (96%)
		300	0.127 (93%)	0.140 (94%)
		400	0.068 (91%)	0.066 (95%)
0.1	0.8	200	0.380 (94%)	0.370 (95%)
		300	0.130 (95%)	0.109 (96%)
		400	0.056 (90%)	0.048 (97%)
0.2	0.5	200	1.214 (94%)	0.580 (97%)
		300	0.727 (95%)	0.326 (96%)
		400	0.500 (93%)	0.217 (97%)
0.2	0.8	200	1.312 (95%)	0.404 (93%)
		300	0.832 (96%)	0.171 (95%)
		400	0.526 (94%)	0.101 (96%)
$\sigma$	$\rho$	n	Exponential (Spike) Model	
			Method 1 (Unweighted Mean) avg. area(coverage)	Method 2 (Weighted Mean) avg.area(coverage)
0.1	0.5	200	0.854 (89%)	0.394 (93%)
		300	0.110 (96%)	0.154 (96%)
		400	0.065 (93%)	0.077 (97%)
0.1	0.8	200	0.208 (92%)	0.215 (94%)
		300	0.081 (93%)	0.085 (97%)
		400	0.040 (91%)	0.048 (96%)
0.2	0.5	200	0.657 (93%)	0.420 (97%)
		300	0.313 (95%)	0.238 (97%)
		400	0.210 (96%)	0.133 (98%)
0.2	0.8	200	0.580 (94%)	0.322 (95%)
		300	0.247 (96%)	0.124 (96%)
		400	0.115 (92%)	0.078 (96%)



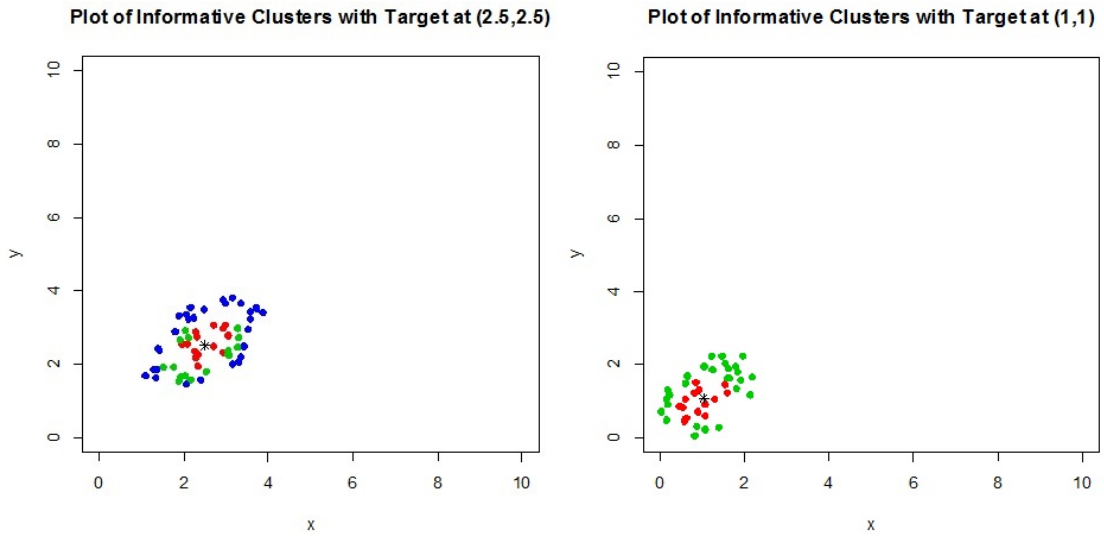


Figure 3.8: Plot of informative clusters for Exponential Signal Model with  $\rho = 0.5$

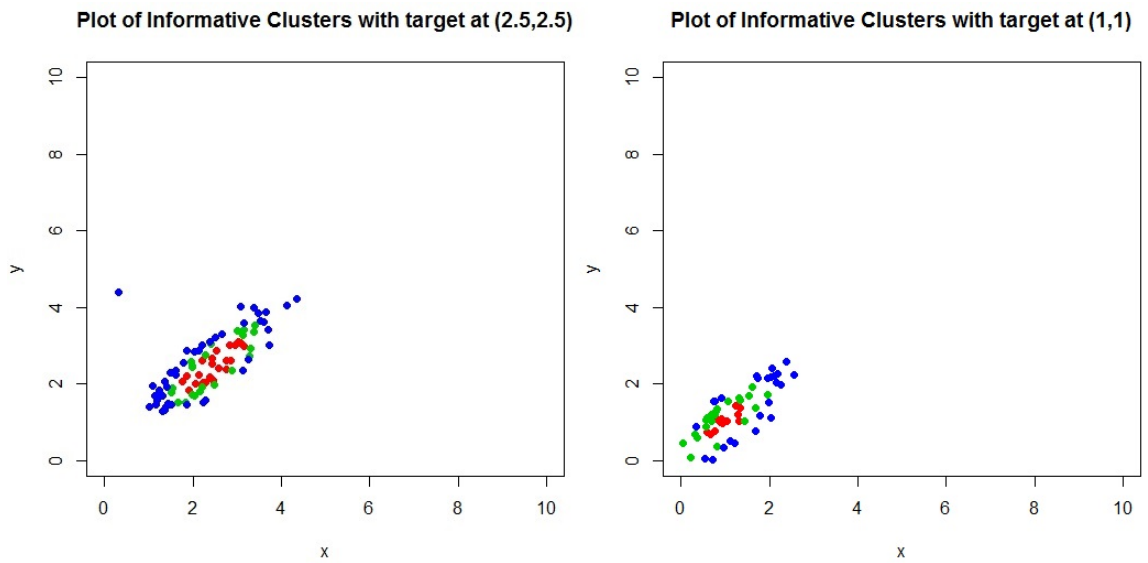


Figure 3.9: Plot of informative clusters for Exponential Signal Model with  $\rho = 0.8$

set-up for the comparative study:

The sensor field is taken to be  $[0, 5] \times [0, 5] \in \mathbb{R}^2$  and three sensor budgets: 200, 300 and 400 are considered. The noise variable  $\epsilon$  is taken to be  $N(0, \sigma)$  with  $\sigma$  assuming values from  $\sigma = 0.3, 0.5$ , which correspond to moderate and high noise levels for the isotropic models. We consider the following isotropic signal models :

1. Exponential model:  $g_0(\|x - \theta_0\|) = 2e^{-\frac{(\|x - \theta_0\|)^2}{2}}$
2. Polynomial model:  $g_0(\|x - \theta_0\|) = \frac{2}{1 + (\|x - \theta_0\|)^3}$
3. Exponential (spike) model:  $g_0(\|x - \theta_0\|) = 2e^{-\frac{(\|x - \theta_0\|)^2}{.4}}$

We use the target location (2.5,2.5) in the middle of the monitored region for comparative study. The tabulated results presented in Table 3.4 are based on 300 replications for all settings considered. The performance metrics employed are: (i) the average area of the final bootstrap/sub-sample confidence region (CR) and (ii) the observed coverage, using percentage of times the resulting confidence region contains the true target location, at a nominal 95% level. We compare the performances of the following methods:

1. One-stage Isotonic Regression Method
2. Two-stage (weighted) Isotonic Regression Method
3. Clustering based Method with fitting ellipses for different clusters of sensors

From the results, we can see that even for the isotropic model, the clustering based

method performs better than the one-stage isotonic method in terms of average area and coverage percentage of the resulting confidence regions. However, for isotropic signal models, the two-stage isotonic regression method works better than the clustering based approach. However, it is worth noting that overall, the clustering based approach performs quite well for isotropic signal models as well.

In addition, while applying the clustering based method for isotropic signal models, we also fit circles instead of ellipses for the sensors corresponding to different clusters and compare the results between the two clustering based methods in Table 3.5. For isotropic signal models, the two clustering based methods perform more or less similarly. The ellipse fitting approach produces more precise confidence regions, whereas the circle fitting approach provides more coverage for the confidence regions, on average. One advantage of the circle fitting approach is that we have to estimate fewer parameters while fitting the circles through sensor points. On the other hand, the ellipse fitting approach would be more robust as it can tackle both isotropic and anisotropic signals and provides quite precise confidence regions even for isotropic signals. Based on the results, it appears that fitting the ellipse is a better option if one suspects potential deviation from isotropy, given the fact that fitting the circles does not appear to give a substantial systematic advantage.

### **3.4 Applications - The ZebraNet Project**

We once again apply the proposed estimation method to track the movement of zebras based on data collected as part of a ZebraNet project at the Sweetwaters Game Reserve near Nanyuki, Kenya during the summer of 2005. As described in previous chapter, the sensors were equipped with GPS location devices and were actually fitted as collars on four zebras, selected for their varying behavioral patterns. The zebras' locations and a time stamp were recorded every few minutes for approximately 10

Table 3.4: Comparison of Methods for Isotropic signal with target at (2.5,2.5)

$\sigma$	n	$n_1$	$n_2$	Exponential Model		
				1-stage Isotonic CR avg. area(coverage)	2-stage Isotonic(wt) CR avg.area(coverage)	Clustering based CR avg. area(coverage)
0.3	200	66	134	0.110 (51%)	0.050 (93%)	0.151 (92%)
	300	100	200	0.083 (55%)	0.031 (95%)	0.097 (96%)
	400	133	267	0.054 (58%)	0.023 (96%)	0.072 (96%)
0.5	200	66	134	0.214 (79%)	0.134 (94%)	0.323 (95%)
	300	100	200	0.168 (73%)	0.082 (94%)	0.273 (92%)
	400	133	267	0.130 (84%)	0.071 (95%)	0.226 (87%)
$\sigma$	n	$n_1$	$n_2$	Polynomial Model		
				1-stage Isotonic CR avg. area(coverage)	2-stage Isotonic(wt) CR avg.area(coverage)	Clustering based CR avg. area(coverage)
0.3	200	66	134	0.102 (44%)	0.035 (92%)	0.228 (92%)
	300	100	200	0.063 (53%)	0.023 (94%)	0.166 (96%)
	400	133	267	0.054 (55%)	0.019 (93%)	0.112 (92%)
0.5	200	66	134	0.265 (77%)	0.108 (95%)	0.420 (96%)
	300	100	200	0.196 (74%)	0.074 (94%)	0.407 (92%)
	400	133	267	0.110 (72%)	0.051 (95%)	0.330 (92%)
$\sigma$	n	$n_1$	$n_2$	Exponential (spike) Model		
				1-stage Isotonic CR avg. area(coverage)	2-stage Isotonic(wt) CR avg.area(coverage)	Clustering based CR avg. area(coverage)
0.3	200	66	134	0.289 (66%)	0.044 (90%)	0.483 (91%)
	300	100	200	0.202 (60%)	0.021 (91%)	0.386 (90%)
	400	133	267	0.076 (62%)	0.013 (93%)	0.350 (88%)
0.5	200	66	134	0.932 (84%)	0.172 (90%)	0.624 (92%)
	300	100	200	0.572 (84%)	0.072 (95%)	0.667 (91%)
	400	133	267	0.240 (83%)	0.027 (94%)	0.582 (96%)

Table 3.5: Comparison of Ellipse and Circle Fitting in Clustering based Method for Isotropic signal with target at (2.5,2.5)

$\sigma$	n	Exponential Model	
		Clustering (Ellipse Fitting) based CR avg. area(coverage)	Clustering (Circle Fitting) based CR avg.area(coverage)
0.3	200	0.151 (92%)	0.213 (96%)
	300	0.097 (96%)	0.114 (95%)
	400	0.072 (96%)	0.087 (94%)
0.5	200	0.323 (95%)	0.423 (94%)
	300	0.273 (92%)	0.297 (94%)
	400	0.226 (87%)	0.243 (92%)
$\sigma$	n	Polynomial Model	
		Clustering (Ellipse Fitting) based CR avg. area(coverage)	Clustering (Circle Fitting) based CR avg.area(coverage)
0.3	200	0.228 (92%)	0.340 (95%)
	300	0.166 (96%)	0.201 (96%)
	400	0.112 (92%)	0.146 (93%)
0.5	200	0.420 (96%)	0.523 (94%)
	300	0.407 (92%)	0.473 (92%)
	400	0.330 (92%)	0.324 (93%)
$\sigma$	n	Exponential (Spike) Model	
		Clustering (Ellipse Fitting) based CR avg. area(coverage)	Clustering (Circle Fitting) based CR avg.area(coverage)
0.3	200	0.483 (91%)	0.714 (93%)
	300	0.386 (90%)	0.561 (96%)
	400	0.350 (88%)	0.427 (95%)
0.5	200	0.624 (92%)	0.852 (97%)
	300	0.667 (91%)	0.734 (94%)
	400	0.582 (96%)	0.685 (96%)

days.

In order to apply the proposed algorithm in this application, the following simulated sensor experiment was designed. The original monitored region is roughly 5km  $\times$  5km; thus, we simulated a random deployment of 400 sensors uniformly distributed in the region  $[0, 5] \times [0, 5]$ , and mapped the true location of a zebra available from the ZebraNet data to this monitored region. We show the localization results for one zebra selected at random and considered its locations over a particular time period.

The emitted signals were generated according to the following polynomial anisotropic model:

$$Y_i = \frac{2}{1 + ((x_i - \theta_0)^T \Sigma^{-1} (x_i - \theta_0))^{3/2}} + \epsilon_i$$

where  $\epsilon_i \sim N(0, \sigma)$  with  $\sigma = 0.2$  to simulate noisy signal readings. We also considered  $\Sigma = \begin{pmatrix} 1 & \rho \\ \rho & 1 \end{pmatrix}$  with  $\rho = 0.5$  for above model. We then apply our proposed method to find a confidence region for the location of the zebra, over a particular time period, using all 400 sensors. We consider six different time points (corresponding to six different target locations) and apply both Method 1 and Method 2 to construct the confidence regions. The locations of the selected zebra at the six chosen time points and their corresponding estimated confidence regions for Method 1 and 2 are depicted in Figures 3.10 and 3.11, where the ellipsoidal grey region is the estimated confidence region and the black dot inside corresponds to the true location of the zebra. The actual locations of the zebra and the area of the estimated confidence regions are provided in Table 3.6. Based on the results, we can see that Method 2 produces more precise confidence regions for the zebra locations than Method 1 in this case. Overall, the proposed clustering based methods show satisfactory performance,

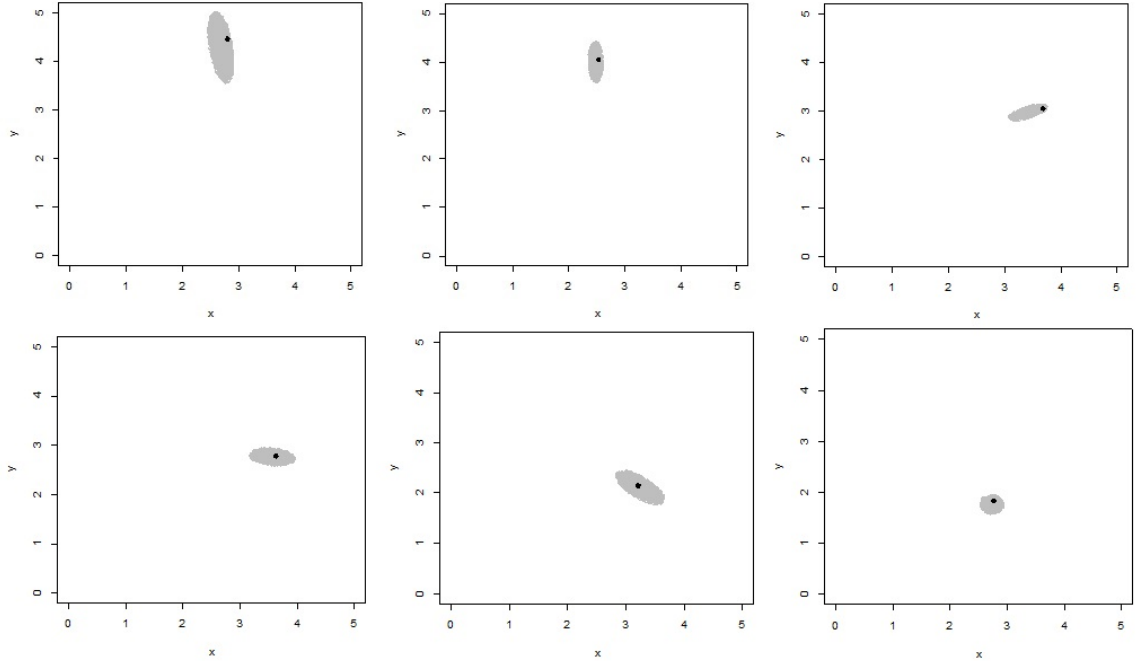


Figure 3.10: Confidence Region of zebra location at six time points, based on Method 1 (Unweighted Mean)

producing fairly precise confidence regions.

Table 3.6: Performance of Clustering method at zebra tracking, based on Polynomial Signal

Zebra Location	Area of Confidence Region (Method 1)	Area of Confidence Region (Method 2)
(2.80, 4.46)	0.40	0.26
(2.53, 4.06)	0.13	0.12
(3.68, 3.05)	0.10	0.04
(3.63, 2.78)	0.17	0.07
(3.21, 2.14)	0.26	0.09
(2.76, 1.83)	0.11	0.07

### 3.5 Theoretical Issues

From the simulation studies and the real life application, we can see that the proposed clustering based method works quite well for anisotropic signal models where

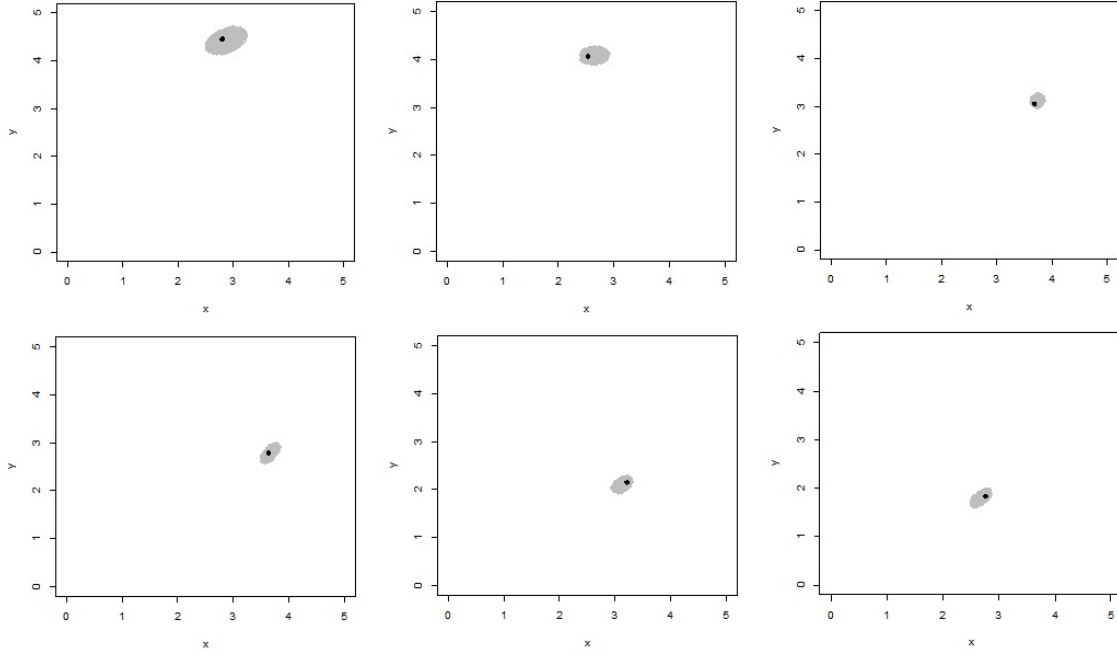


Figure 3.11: Confidence Region of zebra location at six time points, based on Method 2 (Weighted Mean)

the signals form elliptical contours. To our knowledge, there has not been any substantial theoretical advancement for target estimation problem for anisotropic model so far. However, for our proposed clustering based method, we have empirical evidence that the parametric estimate has a  $\sqrt{n}$  convergence rate and also have asymptotic normal distribution. The relevant figures and plots are provided in Appendix C at the end. Note that we do not have to directly estimate the unknown signal function  $g_0$  in this approach, we can directly estimate the target location using the geometry of elliptical contours generated by the true signal function  $g_0$ . Using this clustering based approach, we can avoid, to some extent, the complexity that arises from estimating  $g_0$  effectively in *bundled* parameter models. In many other *bundled* parameter problems, the performance of the parametric estimate relies heavily on the effectiveness of the corresponding non-parametric estimate. The theoretical properties of the proposed clustering based method will be a topic of future study.



## CHAPTER IV

# Kernel-based Target Estimation for Isotropic Signal

### 4.1 Introduction

In this Chapter, we revisit the problem of estimating the target location for isotropic signals and propose a smooth estimate of the unknown signal function  $g_0$ , as well as a modified estimate of the unknown target location  $\theta_0$ . Recall that in Chapter II, we proposed an isotonic regression based method to estimate the target location for isotropic signal models, but the estimate of  $g_0$  obtained by isotonic regression is not a smooth function, making theoretical analysis difficult for the parameters. In this chapter, starting with the isotonic estimate obtained using the method described in Chapter II as an initial estimate, we consider a modified estimate of the signal function  $g_0$  using a kernel-based method and subsequently obtain a modified estimate of  $\theta_0$ .

Recall that for the isotropic signal model, the signal strength received by the sensor is a decreasing function of the distance between the target and the sensor, the signal received can then be modeled as:  $Y_i = g_0(\|x_i - \theta_0\|) + \epsilon_i, i = 1, 2, \dots, n$ , where  $x_i$  is the known location of  $i$ -th sensor,  $\theta_0$  is the unknown location of the target and  $g_0$  is an unknown monotone decreasing function. As before,  $\epsilon_i, i = 1, 2, \dots, n$  are the

i.i.d random noises. Our primary goal is to estimate  $\theta_0$ , which will also necessitate some estimation of  $g_0$ . As explained before, in this particular model, the parametric part  $\theta_0$  and the non-parametric part  $g_0$  are *bundled* together, that is, they are not *well-separated* as  $\theta_0$  sits inside the function  $g_0$  as an argument, which makes the estimation method more challenging.

Other examples of *bundled* parameters include linear regression model for censored survival data where the unspecified error distribution function is a function of the regression coefficients, single index model or Cox regression model where the unspecified link function has regression coefficients as part of its argument. There is a rich literature on asymptotic distribution theory for semiparametric M-estimation in a variety of different models where the parametric and non-parametric components are separated, see for example He et. al.(2010), Huang (1996, 1999), Wellner et. al.(2007), but few theoretical advancements have been made for semiparametric models where the two parameters are *bundled* together.

However, in recent years, there have been some significant advancements on the theoretical front for semiparametric *bundled* parameter problems. In their paper, Ichimura and Lee (2010) have studied the asymptotic properties of semiparametric M-estimators and have shown that the asymptotic distribution of the parametric estimate is Gaussian under certain regularity conditions on the estimate of the non-parametric part. For most of their models, they have considered a smooth estimate of the non-parametric component such that the regularity conditions are satisfied, leading to asymptotic normality of the parametric estimate. Also, Ding and Nan (2012) have used a spline based approach for estimation in the semiparametric linear regression model with right censored data and have established asymptotic normality of the parametric component, under certain regularity conditions. These recent devel-

opments motivate us to consider a smooth estimate of the non-parametric component  $g_0$  for our model, so that further theoretical investigations about the parametric estimate, as well as the non-parametric one can be facilitated.

## 4.2 Estimation Methods in One-dimension

Recall the semi-parametric model introduced in the previous section:

$$Y_i = g_0(\|x_i - \theta_0\|) + \epsilon_i, i = 1, 2, \dots, n$$

. To estimate  $\theta_0$ , we propose the following kernel-based estimation method, starting from the initial isotonic estimate obtained by the method in Chapter II:

1. Let  $(\tilde{\theta}, \tilde{g})$  be the initial isotonic estimate for  $(\theta_0, g_0)$ , based on the isotonic estimate method described in Chapter II.
2. Next, we update the step function  $\tilde{g}$  to a smooth one using the following kernel smoothing idea:

$$\hat{g}(u) = \frac{\sum_{i=1}^n K\left(\frac{u-u_i^*}{h_n}\right) Y_i^*}{\sum_{i=1}^n K\left(\frac{u-u_i^*}{h_n}\right)}$$

where  $u_i^* = |x_i - \tilde{\theta}|$  and  $Y_i^* = \tilde{g}(u_i^*)$ ,  $K(\cdot)$  is a kernel function and  $h_n$  is a specific bandwidth.

3. Finally,  $\tilde{\theta}$  is updated via

$$\hat{\theta} = \arg \min_{\theta} \sum_{i=1}^n (Y_i - \hat{g}(|X_i - \theta|))^2$$

As  $\hat{g}$  is a smooth function, we can solve the above minimization problem using Newton-Raphson method, using the derivative of the above objective functions w.r.t

$\theta$  and  $\hat{g}$ .

4. Repeat steps (2)-(3) until the solution converges.

### 4.3 Performance Evaluation

We evaluated the performance of the above kernel based method for one-dimensional signal models and compared it to the performance of the two-stage isotonic regression based method described in Chapter II. The following one-dimensional signal models were considered:

1. Exponential model:  $g_0(|x - \theta_0|) = 2e^{-\frac{(|x - \theta_0|)^2}{2}}$
2. Polynomial model:  $g_0(|x - \theta_0|) = \frac{2}{1 + (|x - \theta_0|)^3}$

We consider the interval  $[0, 5]$  for the simulation study and consider two locations,  $\theta_0 = 2.5$  and  $\theta_0 = 1$  to demonstrate the results. The noise variable  $\epsilon$  is taken to be  $N(0, \sigma)$  with  $\sigma$  assuming values  $\sigma = 0.1, 0.3, 0.5$  for three different noise levels for our models. We use Gaussian kernel and cross-validation to select the optimal bandwidth for the kernel-based method.

The tabulated results given in Tables 4.1 and 4.2 are based on 200 replications for all settings considered. We compare the bias and MSE's of the estimates obtained by isotonic regression based estimation method and the kernel-based estimation method. Based on the results, we can see that overall, these two methods performed similarly, with isotonic regression based method doing slightly better in some cases, w.r.t. MSE's. Though the modified kernel based method is not able to outperform the isotonic regression based method described in Chapter II, it might be easier to investigate theoretical properties of the parametric estimate of  $\theta_0$  in this case.

Table 4.1: 1-dim Simulation Results with target at (2.5)

$\sigma$	n	Exponential Model			
		Isotonic Method		Kernel Method	
		Bias	MSE	Bias	MSE
0.1	100	0.0005	0.0006	-0.0002	0.0004
	200	-0.0003	0.0002	0.0018	0.0003
0.3	100	-0.0050	0.0020	-0.0035	0.0030
	200	0.0008	0.0011	-0.0048	0.0017
0.5	100	0.0060	0.0066	-0.0011	0.0089
	200	-0.0008	0.0040	0.0025	0.0060
$\sigma$	n	Polynomial Model			
		Isotonic Method		Kernel Method	
		Bias	MSE	Bias	MSE
0.1	100	-0.0015	0.0006	-0.0064	0.0008
	200	-0.0013	0.0002	-0.0007	0.0003
0.3	100	-0.0035	0.0021	-0.0150	0.0048
	200	0.0008	0.0009	-0.0017	0.0032
0.5	100	-0.0120	0.0052	-0.0224	0.0130
	200	-0.0028	0.0036	-0.0018	0.0096

#### 4.4 Theoretical Issues and Conclusion

As mentioned before, the main motivation to consider smooth estimate of  $g_0$  for our semiparametric model comes from the recent works of Ichimura and Lee (2011), Ding and Nan (2012), where they were able to establish asymptotic normality of the parametric component using a smooth estimate of the non-parametric one. Even though the kernel-based estimation method performs more or less similarly to the isotonic regression based method, it would be easier to investigate the theoretical properties of the parametric estimate in this case as it is computed based on a smooth estimate of the non-parametric component  $g_0$ . With these recent developments in the field of semiparametric *bundled* parameter literature, theoretical properties of the current kernel-based estimate of  $\theta_0$  for our model will be a topic for future study, also the performance of the method should be evaluated for two-dimensional scenarios as well.

In this thesis, we have proposed some computationally attractive methods for tar-

Table 4.2: 1-dim Simulation Results with target at (1)

$\sigma$	n	Exponential Model			
		Isotonic Method		Kernel Method	
		Bias	MSE	Bias	MSE
0.1	100	0.0100	0.0006	-0.0210	0.0005
	200	0.0025	0.0002	0.0910	0.0084
0.3	100	-0.0020	0.0064	-0.0219	0.0048
	200	0.0100	0.0024	0.0760	0.0074
0.5	100	-0.0400	0.0364	-0.0597	0.0351
	200	-0.0325	0.0119	0.0670	0.0083

$\sigma$	n	Polynomial Model			
		Isotonic Method		Kernel Method	
		Bias	MSE	Bias	MSE
0.1	100	0.0100	0.0006	0.0500	0.0030
	200	0.0075	0.0002	0.0667	0.0052
0.3	100	-0.0350	0.0083	0.0369	0.0066
	200	0.0200	0.0007	0.0767	0.0074
0.5	100	-0.0300	0.0178	0.0522	0.0143
	200	0.0025	0.0034	0.0831	0.0110

get detection in a semiparametric modeling set-up, but there is ample scope of future theoretical/computational work which should be an interesting topic of study for future researchers. The development of these new methodologies opens up a number of avenues for deep theoretical investigation and hopefully will lead to more improved/efficient methodologies for target estimation in wireless sensor networks.

## APPENDICES

## APPENDIX A

### Isotonic Regression

In equation (2.2), we are minimizing the following for fixed  $\theta$ :

$$g_\theta = \arg \min_g S(\theta, g) = \arg \min_g \sum_{i=1}^n (Y_i - g(\|x_i - \theta\|))^2$$

subject to the restriction that  $g$  is a monotone decreasing function. To find the minimizer, we first order the  $\|x_i - \theta\|$  values. Without loss of generality, we assume:

$\|x_1 - \theta\| \leq \|x_2 - \theta\| \leq \dots \leq \|x_n - \theta\|$ . Since  $g$  is monotone decreasing,  $g(\|x_1 - \theta\|) \geq g(\|x_2 - \theta\|) \geq \dots \geq g(\|x_n - \theta\|)$ . The problem is therefore one of minimizing  $\sum_{i=1}^n (Y_i - u_i)^2$  over all  $n$  dimensional vectors  $(u_1, u_2, \dots, u_n)$  satisfying  $u_1 \geq u_2 \geq \dots \geq u_n$ . This is the so-called *isotonic regression* problem that can be solved using the well-known Pool Adjacent Violators Algorithm (PAVA) (see Robertson et al. (1988)) in this case. The solution  $(\hat{u}_1, \dots, \hat{u}_n)$  assumes constant values on blocks of indices producing a piecewise constant function  $g_\theta$ .



## APPENDIX B

### Plots for One-stage Isotonic Estimate

Figure B.1: Histogram and QQplot of  $\sqrt{n}(\hat{\theta} - \theta_0)$  for 1d Exponential Model,  $n=2000$

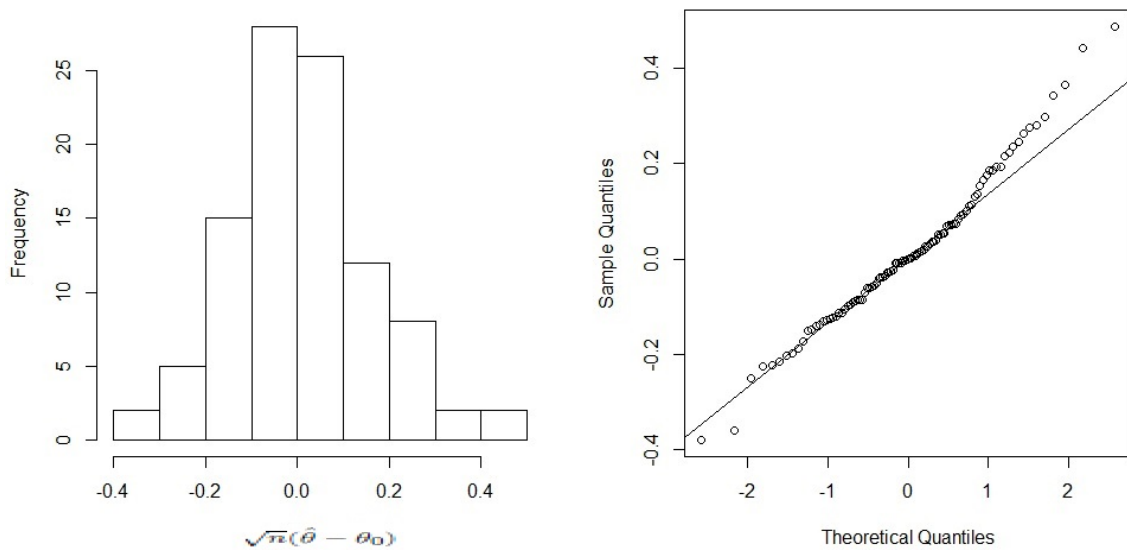
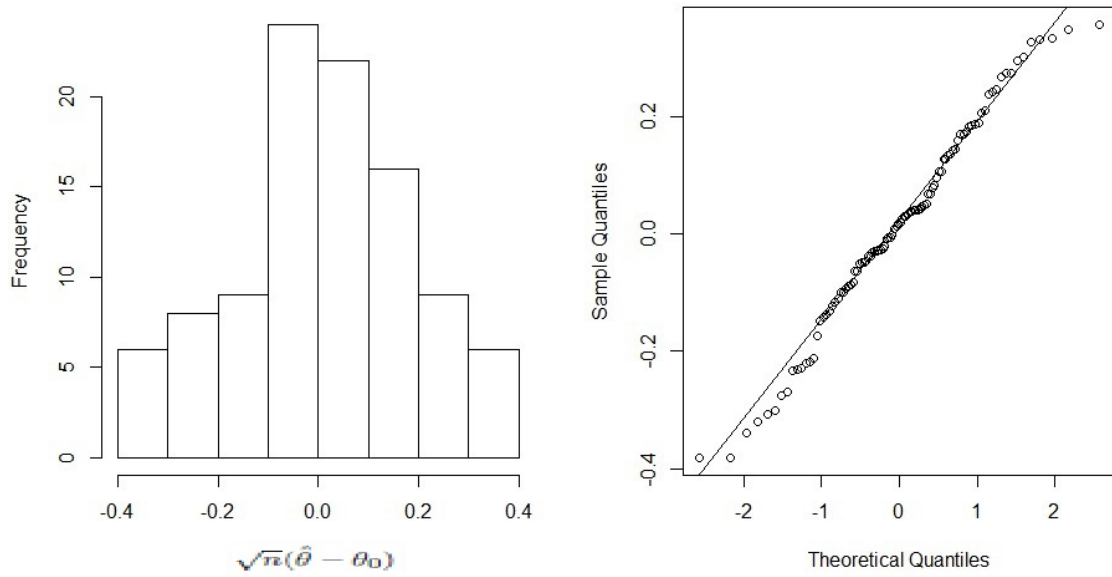


Figure B.2: Histogram and QQplot of  $\sqrt{n}(\hat{\theta} - \theta_0)$  for 1d Polynomial Model,  $n=2000$



## APPENDIX C

### Plots for Clustering based Estimate for Exponential Model

Figure C.1: Histogram and QQplot of  $\sqrt{n}(\hat{\theta}_1 - \theta_{10})$  for 2d Exponential Model,  $n=5000, \rho = 0.5$

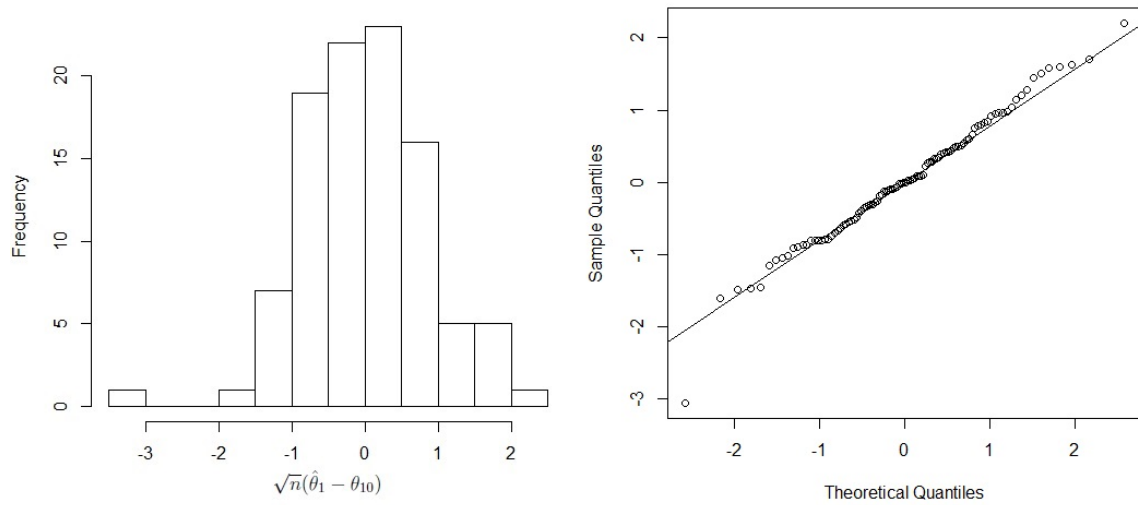
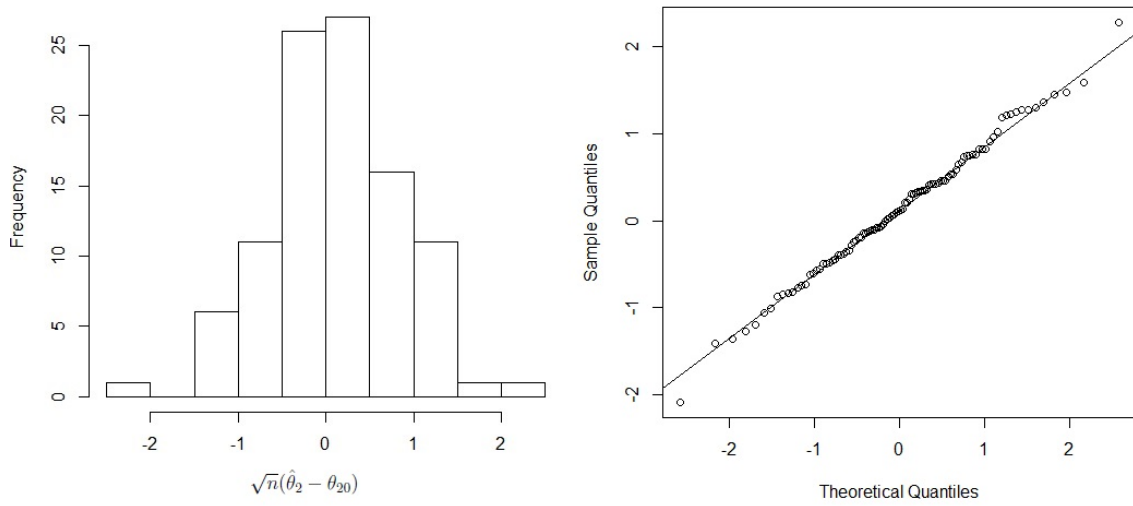


Figure C.2: Histogram and QQplot of  $\sqrt{n}(\hat{\theta}_2 - \theta_{20})$  for 2d Exponential Model,  $n=5000, \rho = 0.5$



## BIBLIOGRAPHY

## BIBLIOGRAPHY

- [1] A. Abdel-Samad, and A. Tewfik (1999), "Search Strategies for Radar Target Localization", in Proceedings of *International Conference on Image Processing*, vol. 3, pp. 862-866.
- [2] G. Anastasi, M. Conti, M. D. Francesco and A. Passarella, "Energy Conservation in Wireless Sensor Networks: A Survey", in *Ad Hoc Networks*, Vol. 7, Issue 3, 537-568, 2009.
- [3] J. Besag, "On the Statistical Analysis of Dirty Pictures". *Journal of the Royal Statistical Society*, Ser. B, 48, 259-302, 1986.
- [4] C. Biernacki, G. Celeux, and G. Govaert, "Assessing a Mixture Model for Clustering with the Integrated Completed Likelihood," *IEEE Transactions on Pattern Analysis and Machine Intelligence*, 22, 719-725, 2000.
- [5] D. Blatt, and A. Hero, "Energy-Based Sensor Network Source Localization via Projection Onto Convex Sets", *IEEE Transactions on Signal Processing*, 54, 3614-3619, 2006.
- [6] K. Bouabdellah, H. Noureddine, S. Larbi, "Using Wireless Sensor Networks for Reliable Forest Fires Detection", *Procedia Computer Science*, 19, 794-801, 2013.
- [7] R. Cardell-Oliver, K. Smettem, M. Kranz, and K. Mayer, "A reactive soil moisture sensor network: Design and Field evaluation", *International Journal of Distributed Sensor Networks*, 1, 149-163, 2005.
- [8] J. Chen, R. Hudson, and K. Yao, "Maximum-Likelihood Source Localization and Unknown Sensor Location Estimation for wideband signals in the near-field", *IEEE Transactions on Signal Processing*, 50, 1843-1854, 2002.
- [9] T. Chen, W. Liao, M. Huang, and H. Tsai, "Dynamic Object Tracking in Wireless Sensor Networks," in *Proceedings of 13th IEEE International Conference on Networks*, vol. 1, p. 6, 2005.
- [10] Y. Ding, and B. Nan, "A Sieve M-theorem for Bundled Parameters in Semiparametric Models, with Application to the Efficient Estimation in a Linear Model for Censored Data". *Annals of Statistics* 39(6): 3032-3061, 2012.

- [11] E. Ermis and V. Saligrama, "Detection and Localization in Sensor Networks Using Distributed FDR", in Proceedings of *Conference on Information Sciences and Systems*, 2006.
- [12] D. Estrin, "Wireless Sensing Systems: from eco-systems to human-systems", in *Feedback and Dynamics in Nature Workshop* held at the Grace Hopper Celebration of Women in Computing Conference, 2006.
- [13] A. Fitzgibbon, M. Pilu and R. B. Fisher, "Direct Least Square Fitting of Ellipses", in *IEEE Journal of Pattern Analysis and Machine Intelligence*, Vol. 21, No. 5, 1999.
- [14] R.D. Gill, "Non- and semi-parametric maximum likelihood estimators and the von-Mises method (part I)". *Scandinavian Journal of Statistics* 16, 97-128, 1989.
- [15] P. Hall, "On projection pursuit regression". *Annals of Statistics*. 17, 573-588, 1989.
- [16] W. Härdle, P. Hall, and H. Ichimura, "Optimal smoothing in single-index models". *Annals of Statistics*. 21, 157-178, 1993.
- [17] N. B. Heidenreich, A. Schindler, S. Sperlich, "Bandwidth selection for kernel density estimation: a review of fully automatic selectors", *Advances in Statistical Analysis*, 97, 403-433, 2013.
- [18] J. L. Horowitz, and W. Härdle, "Direct semiparametric estimation of single-index models with discrete covariates". *Journal of the American Statistical Association*. 91, 1632-1640, 1996.
- [19] W. Hu, N. Bulusu, C. T. Chou, S. Jha, A. Taylor, and V. Tran, "Design and evaluation of a hybrid sensor network for cane toad monitoring," *ACM Transactions on Sensor Networks*, 5, 1-28, 2009
- [20] J. Huang, "Efficient estimation for the Cox model with interval censoring". *Annals of Statistics* 24, 540-568, 1996.
- [21] J. Huang, and J.A. Wellner, "Efficient estimation for the Cox model with Case 2 interval censoring". preprint.
- [22] H. Ichimura, and S. Lee, "Characterization of the asymptotic distribution of semiparametric M-estimators", *Journal of Econometrics* 159, 252-266, 2010.
- [23] H. Ichimura, "Semiparametric least squares (SLS) and weighted SLS estimation of single-index models," *Journal of Econometrics* 58, 71-120, 1993.
- [24] S. S. Iyengar, and R. R. Brooks, "Distributed Sensor Networks: Sensor Networking and Applications", Chapman Hall/CRC, 2012.

- [25] L. Kaplan, Q. Le, and P. Molnar (2001), "Maximum-Likelihood Methods for Bearings-Only Target Localization", in Proceedings of *IEEE International Conference on Acoustics, Speech, and Signal Processing*, vol. 5, pp. 3001-3016.
- [26] N. Katenka, E. Levina, and G. Michailidis, "Local Vote Decision Fusion for Target Detection in Wireless Sensor Networks," *IEEE Transactions on Signal Processing*, 56, 329-338, 2008.
- [27] N. Katenka, E. Levina, and G. Michailidis, "Robust Target Localization from Binary Decisions in Wireless Sensor Networks," *Technometrics*, 50, 448-461, 2008.
- [28] N. Katenka, E. Levina, and G. Michailidis, "Tracking Multiple Targets Using Binary Decisions from Wireless Sensor Networks", forthcoming in *Journal of the American Statistical Association*.
- [29] M. Keller, J. Beutel, A. Meier, R. Lim, and L. Thiele, "Learning from Sensor Network Data," in *Proceedings of the 7th ACM Conference on Embedded Networked Sensor Systems*, New York, NY, USA: ACM, pp. 187-191, 2009.
- [30] J. Kim, and D. Pollard, "Cube Root Asymptotics", *The Annals of Statistics*, 18, 191-219, 1990.
- [31] S. Kim, S. Pakzad, D. Culler, J. Demmel, G. Fenves, S. Glaser, and M. Turon, "Wireless sensor networks for structural health monitoring", in *Proceedings of the 4th international conference on Embedded networked sensor systems*, New York, NY, USA: ACM Press, pp. 427-428, 2006.
- [32] D. Li, K. Wong, Y. Hu, and A. Sayeed, "Detection, Classification, and Tracking of Targets", *IEEE Signal Processing Magazine*, 19, 17-29, 2002.
- [33] A. Mainwaring, J. Polastre, R. Szewczyk, D. Culler, and J. Anderson, "Wireless sensor networks for habitat monitoring", in *Proceedings of the 1st ACM international workshop on Wireless sensor networks and applications*, New York, NY, USA: ACM Press, pp. 88-97, 2002.
- [34] C. Meesookho and S. Narayanan, "Distributed Range Difference Based Target Localization in Sensor Network", in Proceedings of the *39th Asilomar Conference on Signals, Systems and Computers*, pp. 205-209, 2005.
- [35] S.A. Murphy, "Likelihood Ratio Based Confidence Intervals in Survival Analysis", *Journal of the American Statistical Association* 90, 1399-1405, 1995.
- [36] S.A. Murphy, and Van der Vaart, "Semiparametric likelihood ratio inference", *Annals of Statistics* 25, 1371-1803, 1997.
- [37] S.A. Murphy, and Van der Vaart, "Observed information in semi-parametric models", *Bernoulli* 5, 381-569, 1999.



- [38] S.A. Murphy, and Van der Vaart, "On Profile Likelihood", *Journal of the American Statistical Association* 95, 449-465, 2000.
- [39] R. Niu and P. Varshney, "Target Location Estimation in Wireless Sensor Networks Using Binary Data", in *Conference on Information Sciences and Systems*, 2004.
- [40] M. Noel, P. Joshi, and T. Jannett, "Improved Maximum Likelihood Estimation of Target Position in Wireless Sensor Networks using Particle Swarm Optimization", in *Proceedings of 3rd International Conference on Information Technology: New Generations*, 2006.
- [41] P. Padhy, K. Martinez, A. Riddoch, H. L. R. Ong, and J. K. Hart, "Glacial Environment Monitoring using Sensor Networks", in *Proceedings of Real-World Wireless Sensor Networks*, ACM Press, 2005.
- [42] J. L. Powell, J. H. Stock, and T. M. Stoker, "Semiparametric estimation of index coefficients". *Econometrica* 57, 1403-1430, 1989.
- [43] M. V. Ramesh, A. V. Vidyapeetham, "Real-Time Wireless Sensor Network for Landslide Detection", in *Proceedings of 3rd International Conference on Sensor Technologies and Applications*, ISBN: 978-0-7695-3669-9.
- [44] T. Robertson, F. T. Wright, R. L. Dykstra, "Order restricted statistical inference". New York: Wiley, 1988.
- [45] X. Sheng and Y. Hu, "Energy Based Acoustic Source Localization", in *Proceedings of 3rd International Workshop on Information Processing in Sensor Networks*, pp. 286-300, 2003.
- [46] H. Singhal, and G. Michailidis, "Optimal Sampling in State Space Models with Applications to Network Monitoring," in *Proceedings of ACM Sigmetrics Conference*, pp. 145-156, 2008.
- [47] K. Sohraby, D. Minoli, and T. Znati, "Wireless sensor networks: technology, protocols, and applications, John Wiley and Sons", ISBN 978-0-471-74300-2, pp. 203209, 2007.
- [48] V.V. Veeravalli, and P. K. Varshney, "Distributed inference in wireless sensor networks," *Philosophical Transactions of the Royal Society A: Mathematical, Physical and Engineering Sciences*, vol. 370, no. 1958, pp. 100-117, 2012.
- [49] R. Viswanathan and P. Varshney, "Distributed detection with multiple sensors: Part I-Fundamentals," *Proc. IEEE*, vol. 85, no. 1, pp. 54-63, 1997.
- [50] H. Wan, T. Zhang, Y. Zhu, (2012), "Detection and localization of hidden radioactive sources with spatial statistical method," *Annals of Operations Research*, 192, 87-104, 2012.

- [51] H. Wang, K. Yao, and D. Estrin, "Information-Theoretic Approaches for Sensor Selection and Placement in Sensor Networks for Target Localization and Tracking", *Journal of Communication and Networks*, 7, 438-448, 2005.
- [52] L. Wang, and L. Yang, "Spline-backfitted kernel smoothing of nonlinear additive autoregression model". *Annals of Statistics*. 35, 2474-2503, 2007.
- [53] L. Wang, and L. Yang, "Spline estimation of single-index models". *Statistica Sinica* 19, 765-783, 2009.
- [54] W. Wang, V. Srinivasan, B. Wang, and K. Chua, "Coverage for Target Localization in Wireless Sensor Networks", in Proceedings on *Information Processing in Sensor Networks*, pp. 118-125, 2006.
- [55] J.A. Wellner, and Y. Zhang, "Two Likelihood-Based Semiparametric Estimation Methods for Panel Count Data with Covariates", *The Annals of Statistics*, Vol. 35, No. 5, 2106-2142, 2007.
- [56] G. Werner-Allen, K. Lorincz, J. Johnson, J. Lees, and M. Welsh, "Fidelity and yield in a volcano monitoring sensor network," in *Proceedings of the 7th Symposium on Operating Systems Design and Implementation*, USENIX Association, pp. 381-396, 2006.
- [57] N. Xu, S. Rangwala, K. Chintalapudi, D. Ganesan, A. Broad, R. Govindan, and D. Estrin, "A wireless sensor network for structural monitoring", in *Proceedings of the 4th international conference on Embedded networked sensor systems*, New York, NY, USA: ACM Press, 2004.
- [58] Y. Yu, and D. Ruppert, "Penalized spline estimation for partially linear single index models". *Journal of the American Statistical Association* 97, 1042-1054, 2002.
- [59] P. Zhang, C. Sadler, S. Lyon, and M. Martonosi, "Hardware Design Experiences in ZebraNet," in *Proceedings of the ACM Conference on Embedded Networked Sensor Systems*, 2004.
- [60] Y. Zou and K. Chakrabarty, "Target Localization Based on Energy Considerations in Distributed Sensor Networks", *IEEE Transactions on Signal Processing*, 5, 51-58, 2003.